SECTION A.I. SITE CHARACTERIZATION
40 CFR 146.82(a)(2), (3), (5), and (6)

MONTEZUMA NORCAL CARBON SEQUESTRATION HUB

Facility Information

Facility name: Montezuma NorCal Carbon Sequestration Hub
IW-A1

Facility contact: Jim Levine, Managing Partner
2000 Powell Street, Suite 920
Emeryville, CA 94608
Phone: (510) 409-1765
Email: jim.levine@upstream.us.com

Well location: Collinsville, Solano County, California
Lat: 38° 5' 7.334" N Long: -121° 51' 30.914" W NAVD 88
Sec 28 T 3 N R 1 E

Table of Contents

List of Tables

List of Figures

List of Appendices

SECTION A.I. SITE CHARACTERIZATION
40 CFR 146.82(a)(2), (3), (5), and (6)

A.I.1 REGIONAL GEOLOGY, AND LOCAL STRUCTURAL GEOLOGY [40 CFR 146.82(A)(3)(VI)]

Regional Geology

The proposed injection site is in southwestern Montezuma hills, an area of modestly elevated topography north of the Sacramento River between the reclaimed Delta islands to the east and southeast, and Grizzly Island and Suisun Bay to the west (Figure A.I-1). The Montezuma hills are at the southwestern end of the Sacramento Valley, a subaerial, intermontane basin between the Coast Ranges to the west and Sierra Nevada to the east. The modern Sacramento Valley evolved from an ancestral Mesozoic-Tertiary marine forearc basin that formed above a long-lived, east-dipping subduction zone beneath western California (Ingersoll and Dickinson, 1981). Over the past approximately 28 million years, plate convergence and subduction have been progressively replaced by transcurrent motion and strike-slip faulting in western California, leading to shoaling of the marine basin, uplift of the Coast Ranges to the west, and a transition to continental fluvial deposition in the Sacramento Valley (Graham et al., 1983, and references therein).

FIGURE A.I-1. SURFACE FAULTS IN THE MONTEZUMA HILLS STUDY AREA

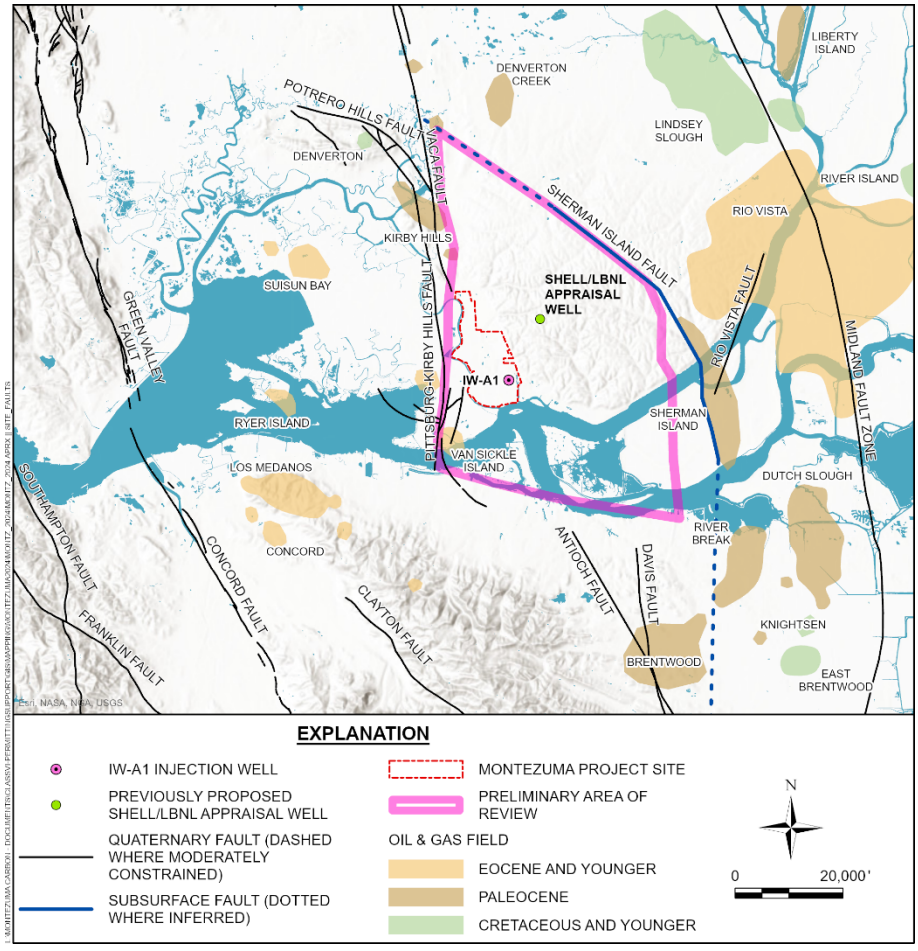

Local Structural Geology

The Montezuma hills approximately coincide with the central part of Rio Vista basin, a north-south-trending extensional sub-basin within the larger forearc basin that formed in early Tertiary time (MacKevett 1992; Krug et al. 1992) (Figure A.I-2). Although the early Tertiary Rio Vista basin is now buried north of the Sacramento River by younger Tertiary and Quaternary terrestrial deposits, an oblique cross-sectional view of the bounding structures and thickened Paleogene marine section in the basin is exposed south of the river in the northeast-dipping backlimb of Mount Diablo anticline. From inspection of this natural, map-scale cross section, the Midland and Kirby Hills fault zones form the eastern and western margins, respectively, of the Rio Vista basin (Figures A.I-1 and A.I-2). Both structures were originally normal faults, and they can be traced in the subsurface of Rio Vista basin southward across the river into the exposed stratigraphic section on the northern flank of Mt. Diablo. The structure correlative to the Kirby Hills Fault south of the river is the Kirker Fault (labeled as "KF" on Figure A.I-7A and south of the study area), which is exposed in the Los Medanos hills between the cities of Pittsburg and Concord.

The Kirby Hills fault zone and the Midland fault comprise the western and eastern structural boundaries, respectively, of an early Tertiary graben in the southwestern Sacramento Valley called the Rio Vista basin (MacKevett, 1992; Krug, 1992; Unruh et al., 2016). East-down normal displacement on the Kirby Hills fault zone and west-down normal displacement on the Midland fault accommodated Paleogene tectonic subsidence of the Rio Vista basin. Normal displacement on the two fault zones died out in the Oligocene, and the Paleogene growth strata of the Rio Vista basin were buried by Neogene continental fluvial deposits. The buried Midland fault has been locally reactivated as a west-side-up reverse fault in the modern transpressional plate tectonic setting of western California, producing uplift and modest eastward tilting of overlying Plio-Pleistocene deposits in the eastern Montezuma Hills (Unruh et al., 2016). Similarly, the modern Pittsburg-Kirby Hills strike-slip fault zone locally reactivates strands of the Paleogene Kirby Hills fault between the town of Pittsburg and the Kirby Hills and Potrero Hills north of the Sacramento River (Unruh and Hector, 1999).

FIGURE A.I-2. EAST-WEST STRATIGRAPHIC CROSS-SECTION THROUGH THE MONTEZUMA HILLS. LIGHT YELLOW FORMATIONS ARE RESERVOIR SANDS

(Based on Krug et al. 1992)

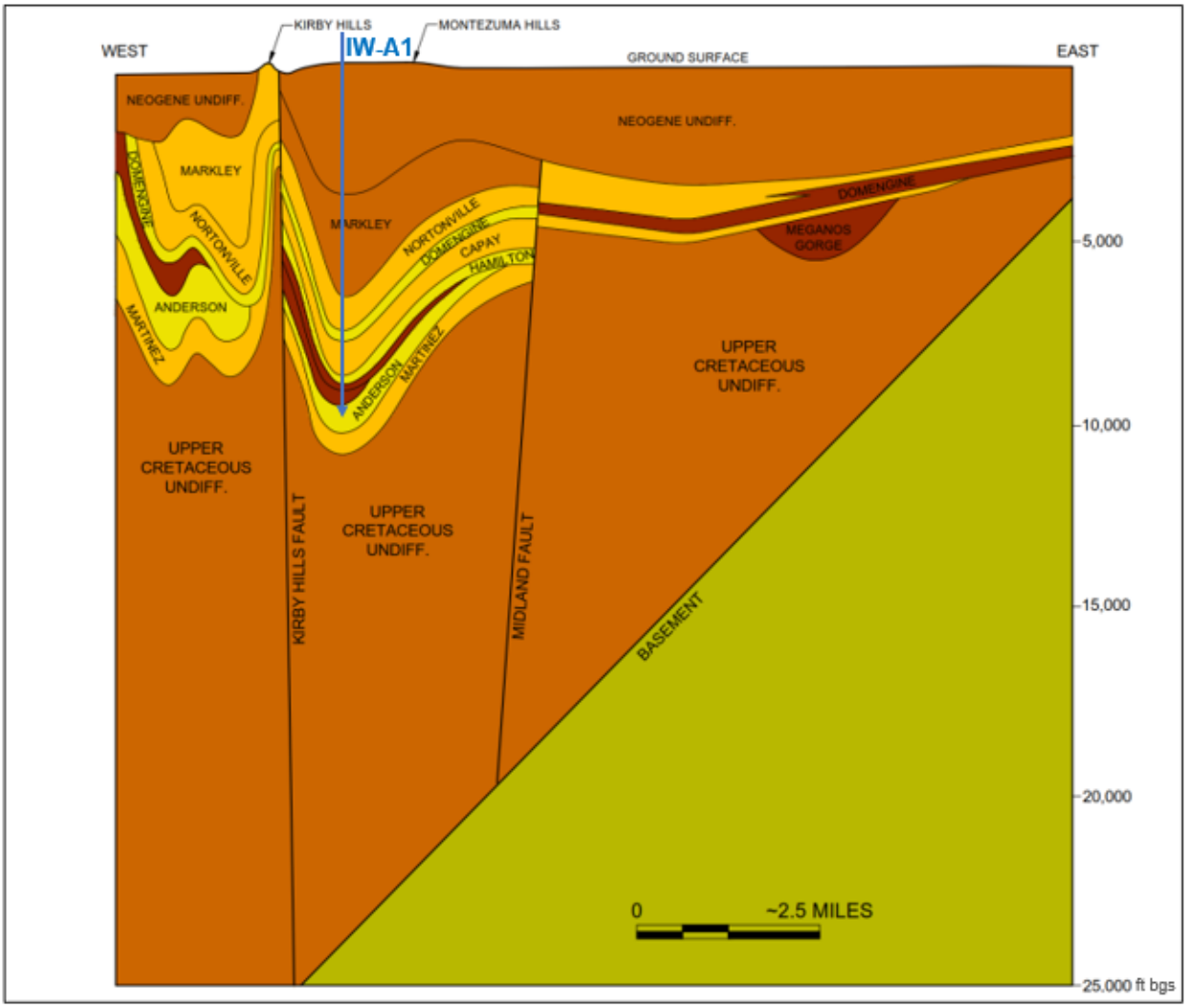

Within the Rio Vista Basin, there is one major fault. The Sherman Island fault is a secondary antithetic normal fault to the Midland fault and terminates westward against the Kirby Hills fault zone (Krug et al., 1992). The Sherman Island fault is mapped west of and subparallel to the Midland fault and interpreted to dip moderately to steeply east (DOGGR, 1982b).

The Paleogene growth section in the Rio Vista basin contains the principal units for injection and confinement. The Anderson sandstone is the planned reservoir for IW-A1, but the Hamilton and Domengine sands are potential future injection intervals as the proposed CO_2 hub expands in size. The confinement zones include the Nortonville Shale (above the Domengine), the Capay Shale (between the Domengine and the Hamilton

sandstones), the Meganos/Upper Martinez shale (between the Hamilton and the Anderson sandstones) and the Lower Martinez shale (below the Anderson). A more detailed description of injection intervals and confining zones is provided in subsequent paragraphs within this template for the application.

Paleogene growth strata in the hanging walls of the main and subsidiary normal faults of the Rio Vista basin are exposed on the northern flank of Mt. Diablo (Sullivan et al., 2021a; 2021b), and support interpretation of open-hole logs and other subsurface data from gas exploration in Rio Vista basin (Pasquini and Milligan 1967; DOGGR, 1982; Krug et al. 1992, and references cited therein) for early Tertiary extension and subsidence in the hanging wall of the ancestral western California subduction zone (Unruh 2021).

Active subsidence of the Rio Vista basin ended in Eocene-Oligocene time. Normal displacement on the bounding Kirby Hills and Midland faults dies out upsection in or below the Oligocene Markley Formation (Figure A.I-2). The forearc basin gradually shoaled in middle to late Tertiary time with the transition from convergent motion to transcurrent motion along the western California plate boundary, and marine conditions were replaced by subaerial fluvial environments. The Paleogene marine strata in Rio Vista basin currently are buried by about 1 km of Neogene and Quaternary deposits.

Plio-Pleistocene uplift, tilting and shortening along the eastern margin of the northern Coast Ranges elevated the Montezuma hills above the surrounding estuarine areas of the Sacramento-San Joaquin Delta, and locally folded and faulted the buried strata of the Rio Vista basin. Folding of the Neogene unit (Figure A.I-2) and structure contours on key Paleogene markers in the Rio Vista basin indicate that at the top of the primary injection zone, the Anderson sand, the proposed borehole locations close to the axis of an asymmetric south-southeast-plunging syncline that is subparallel to and about 5-7 km east of the Kirby Hills fault (Figure A.I-3). The syncline axis trends south toward the southern tip of the Montezuma hills. The top of granitic or Franciscan basement is estimated to be greater than 6 km.

As shown in Figure A.I-3, the area bounded by the Sherman Island Fault to the East and North, the Kirby Hills fault zone to the west, and the Antioch fault to the south bound a deep syncline. These faults juxtapose the injection zone sands against shales and are traps for gas fields along the faults. The trapping nature of these large faults indicate that they are no-flow boundaries and represent the boundary of our AoR. Note that parts of the Antioch fault interpretation and the intersection of the Sherman Island fault with the Kirby Hills fault zone have not been imaged and will be updated with a 3D seismic survey prior to drilling the stratigraphic test well.

In the following paragraphs we provide more detail on these gas fields, which provide important geologic control and information about the AoR. We have also included a short description of the Rio Vista field, because it is one of the largest gas fields in the country and provides useful data on the reservoir and confining zones.

Rio Vista: The Rio Vista gas field lies on the Midland fault and is one of the largest gas fields in the country, having produced the equivalent of over 100 MMtonnes of natural gas, primarily from the Hamilton and Domengine sands. The withdrawal of gas has left reservoir pressures near the Midland fault at the Rio Vista field at generally less than 10% of virgin pressures, although unproduced sands are still at virgin pressure indicating no pressure communication across the confining shales. The Midland fault acts as part of the trapping mechanism on the west side of the Rio Vista field from which most of the gas (>3.5 TCF) has been produced. While the drive mechanism on the west side is gas drive, on the east side the mechanism is water drive and no pressure depletion is observed again indicating that the Midland fault is a no flow/pressure boundary.

Kirby Hills: The Kirby gas field is the closest gas field north of the proposed location. The center of this field is roughly 6 miles north of IW-A1, producing natural gas from the Domengine and Anderson zones. These intervals are trapped against the Kirby Hills fault, which juxtaposes Upper Cretaceous shales to the west against the reservoir zones. Kirby Hills is currently being used as a gas storage field. During gas withdrawal, reservoir pressures drop to less than 500 psi and during injection they rise to over 2000 psi. At Kirby Hills, measured permeability in the Anderson (~5500 feet [ft] subsea) was between 30 and over 600 mD although we expect compaction effects with depth to reduce the permeability in the Anderson interval to about 20 mD at IW-A1.

Sherman Island: The Sherman Island field was created by an antithetic normal fault to the Midland Fault, down-dropped on the northeast side of the fault. The fault again acts as part of the seal as the Midland Fault does at Rio Vista and at Kirby Hills.

Van Sickle Island: The Van Sickle Island gas field has 20 wells in it, 16 of which are only 1-2 miles west of IW-A1. A typical gas well in this field is between 7,500 and 8,000 feet below ground surface (ft bgs) and produced gas from the Domengine at that depth. As with the other fields, the Kirby Hills fault possibly splays to form part of the trap.

There are also some key dry holes closer to IW-A1 than these fields that provide important geologic control.

Brazos Oil and Gas "Concord Gun Club": Drilled in 1951 to a depth of 7,003 ft bgs. The well bottomed in the Markley Formation, and thus did not reach any of the zones of interest. The documentation for this well states that the base of freshwater might be 1,800 or 1,900 ft bgs. This well is shown as 09500423 on Figure A-3A of the Application Narrative.

Hershey Oil "McDougal": Cut the Kirby Hill fault near total depth, ending up in Upper Cretaceous Forbes formation rocks (MacKevett, 1992). This well is shown as 0409520724 on Figure A-3A of the Application Narrative.

McCulloch Oil "GP 1-7" and "Anderson 1-5": These wells lie between IW-A1 and the Sherman Island fault. The Anderson 1-5 well is important because it drilled over 14,000 ft subsea and bottomed in the Upper Cretaceous, thus seeing all the potential relevant geologic units of potential interest. The "GP" well went to 11,000 ft subsea and also penetrated all zones of interest. The GP1-7 well is shown as 0409520436 on Figure A-3A of the Application Narrative. The "Anderson 1-5" well is shown as 09520430 on Figure A-3A of the Application Narrative.

Further north and within or near the center of the syncline are a group of deep wells. These were drilled at depths of 10,000 ft subsea to over 12,000 ft subsea Krug, et.al. (1992) show in their paper that these wells were drilled on the western side of the syncline. These wells give good control on the thickness of the Anderson zone across the AoR.

Seismic Data

The geologic suitability of the MC project area was previously evaluated by Shell and LBNL as part of a US DOE-supported pilot CO_2 injection project to handle the CO_2 from Shell's refinery in Martinez (Hymes 2010). The pilot project included drilling and formation property testing followed by injection and monitoring of a small amount of CO_2. Based upon those previous efforts, Shell concluded that the site geology was very attractive, with the ability to safely store large volumes of CO_2. Shell's target injection interval was also the Anderson unit although they noted that the Hamilton and Domengine were also attractive. Members of LBNL staff that contributed to this report have also played a significant role in the Class VI EPA application.

To correlate the stratigraphy, an injection well location was placed roughly 3 miles north of the proposed IW-A1 well based on an old 2-D seismic line (Figure A.I-3). This seismic line was obtained from Hymes (2010) and is representative of a zone approximately 3 miles due north of well IW-A1. The wells are superimposed onto the image for reference. The Sherman Island Fault is displayed, as well as an unnamed fault to the east. The cross section spans multiple miles horizontally. The continuous nature of the unit

boundaries can be seen as well as the absence of faulting near IW-A1. Also note the thickening between the Hamilton and Massive horizons.

FIGURE A.I-3. 2-D SEISMIC DATA WITH IW-A1 INJECTION WELL PROJECTED NORTH ALONG STRIKE

(From Hymes [2010])

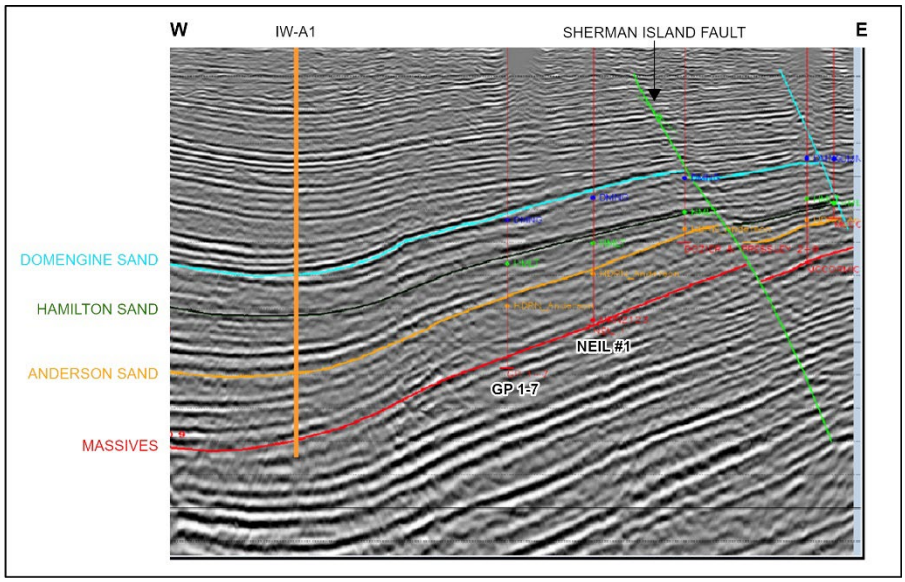

A.I.2 MAPS AND CROSS SECTIONS OF THE AoR [40 CFR 146.82(A)(2), 146.82(A)(3)(I)]

As described above and in Figures A.I-1 through A.I-5, the Area of Review (AoR) is bounded by large faults that are known to be no flow boundaries in gas fields along the faults. Note that there is limited data within parts the AoR, particularly near IW-A1. Once 3D seismic data is available and MW-A1 is evaluated, these maps will be updated. Note that the areal extent of all the formations extend to the boundaries of the AoR. See the Area of Review and Corrective Action Plan for additional maps and cross sections of the AoR.

A.I.3 FAULTS AND FRACTURES [40 CFR 146.82(A)(3)(II)]

A detailed description including maps and cross-sections of the MC site and the associated geologic faults and associated regional structures is provided in the preceding sections of this template document for this application.

A.I.4 INJECTION AND CONFINING ZONE DETAILS [40 CFR 146.82(A)(3)(III)] AND PETROPHYSICAL INFORMATION [40 CFR 146.82(A)(3)(IV)],

Figure A.I-4 shows the predicted formations along with their approximate depths/thicknesses near the IW-A1 location. Information used to generate Figure A.I-4 included the following wells (see Figure A-3A in the Project Narrative for locations and Table B-1 of the Area of Review and Corrective Action Plan for completion information): Anderson 1-5 (API 09520430), GP 1-7 (API 09520436), McDougal 2-8 (API 09520724), and Swepi-Hershey State 1-8 (API 09520674). Information also included MacKevett (1992). Figures A.I-5A through A.I-5I provide preliminary contour maps of formation tops that will be updated with 3D seismic data collected for this project. Information about the potential storage reservoirs comes from data sheets for Van Sickle, Kirby Hills, Sherman Island, and Rio Vista gas fields where these formations have produced (State of California, Division of Oil and Gas, Volume 3: Oil and Gas Fields) as well as articles. These data are considered representative because the geology correlates well between the fields, indicating that the geology within the AoR is likely similar. Information about the confining zones comes from various articles.

FIGURE A.I-4. GENERAL STRATIGRAPHIC COLUMN FOR MC PROJECT AREA

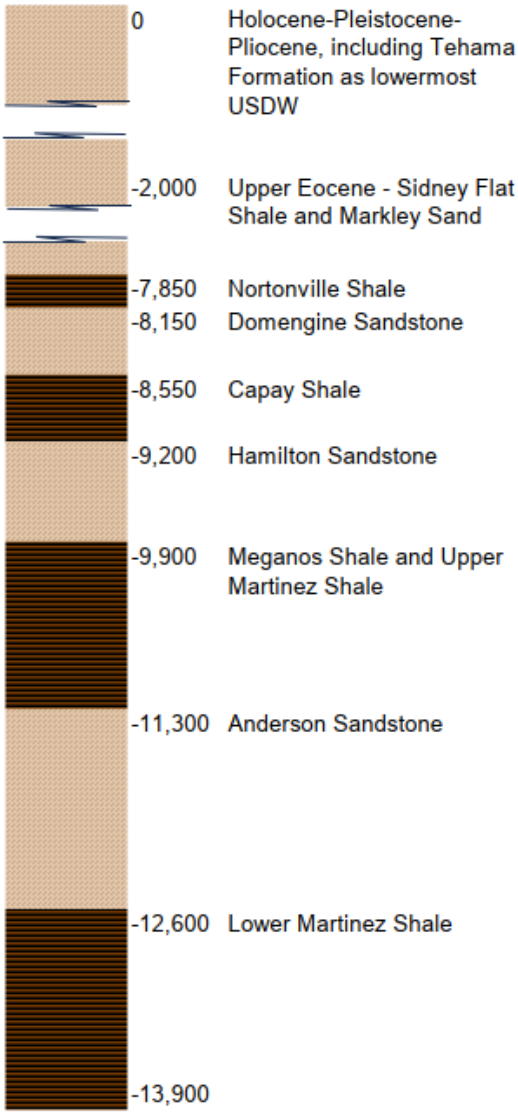

FIGURE A.I-5A. AoR BOUNDARY AND STRUCTURAL CONTOURS – TOP OF NORTONVILLE SHALE

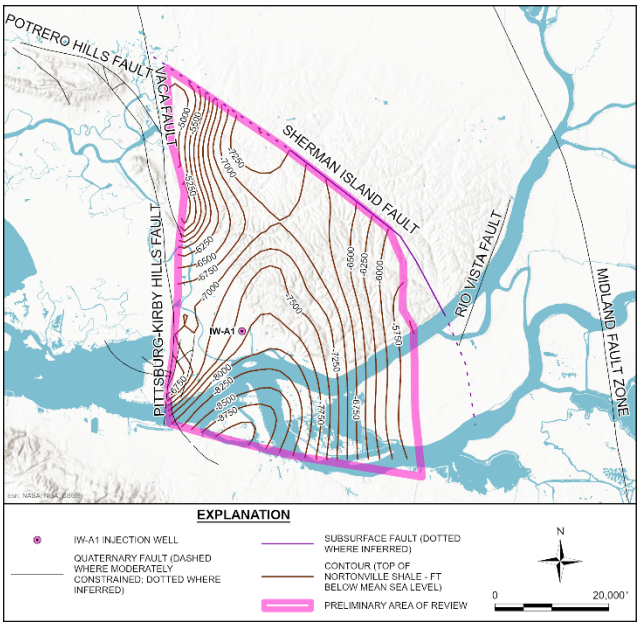

FIGURE A.I-5B. AoR BOUNDARY AND STRUCTURAL CONTOURS – TOP OF DOMENGINE SANDSTONE

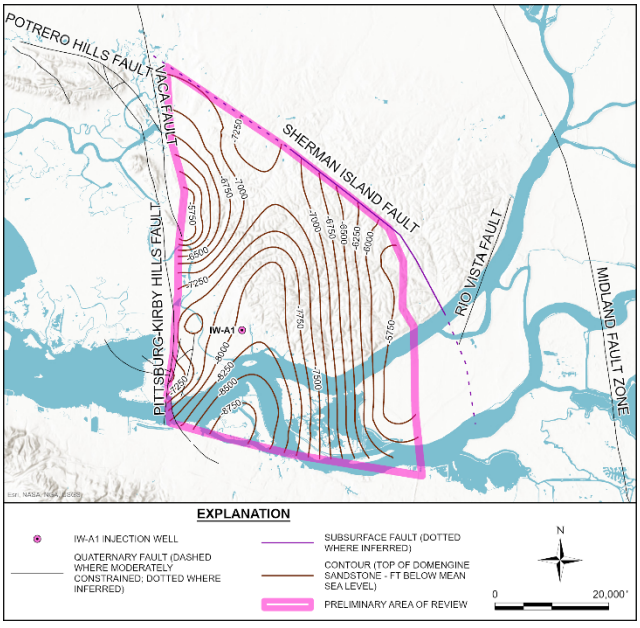

FIGURE A.I-5C. AoR BOUNDARY AND STRUCTURAL CONTOURS – TOP OF CAPAY SHALE

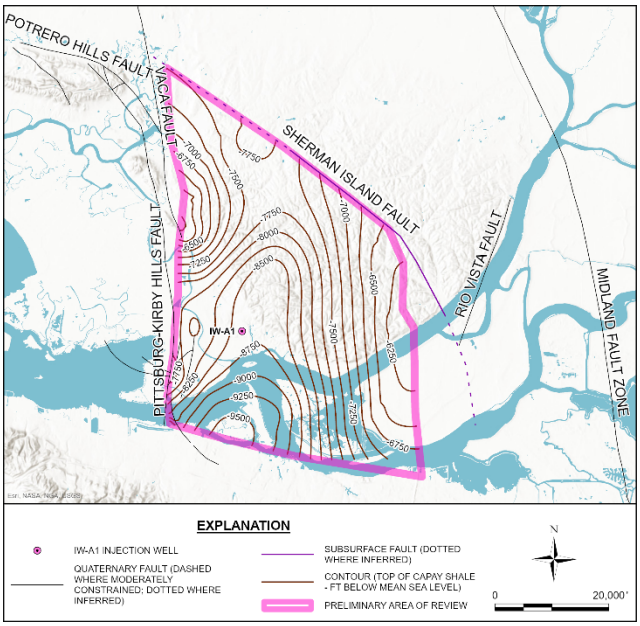

FIGURE A.I-5D. AoR BOUNDARY AND STRUCTURAL CONTOURS – TOP OF HAMILTON SANDSTONE

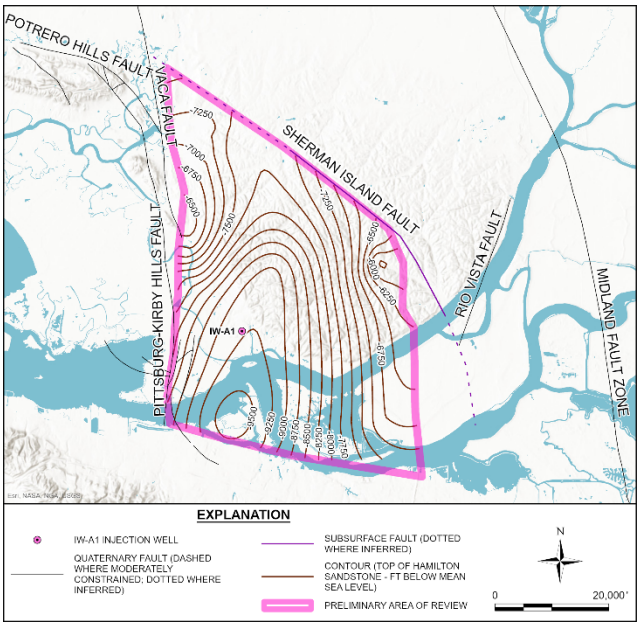

FIGURE A.I-5E. AoR BOUNDARY AND STRUCTURAL CONTOURS – TOP OF MEGANOS SHALE

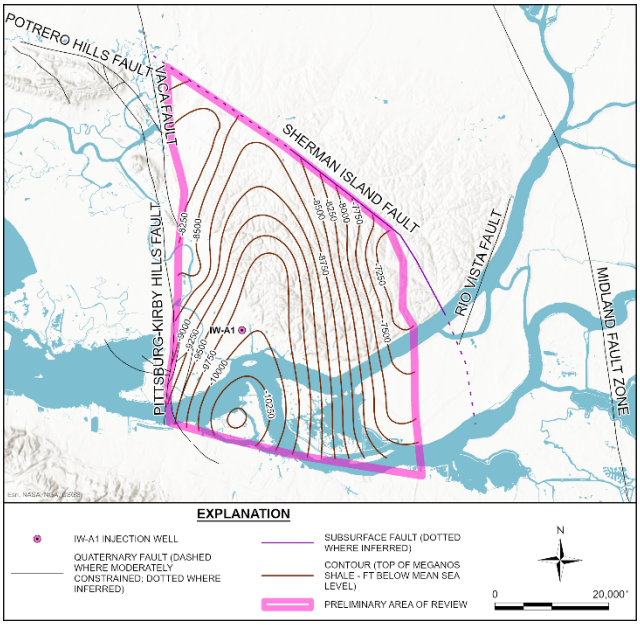

FIGURE A.I-5F. AoR BOUNDARY AND STRUCTURAL CONTOURS – TOP OF UPPER MARTINEZ SHALE

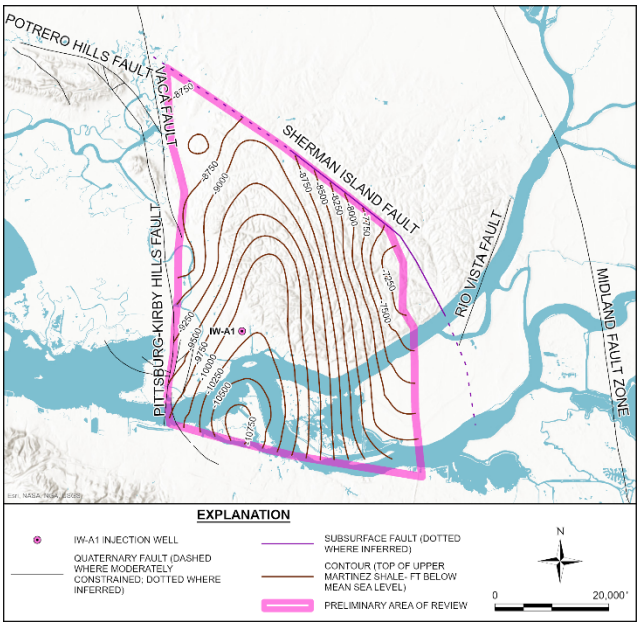

FIGURE A.I-5G. AoR BOUNDARY AND STRUCTURAL CONTOURS – TOP OF ANDERSON SANDSTONE

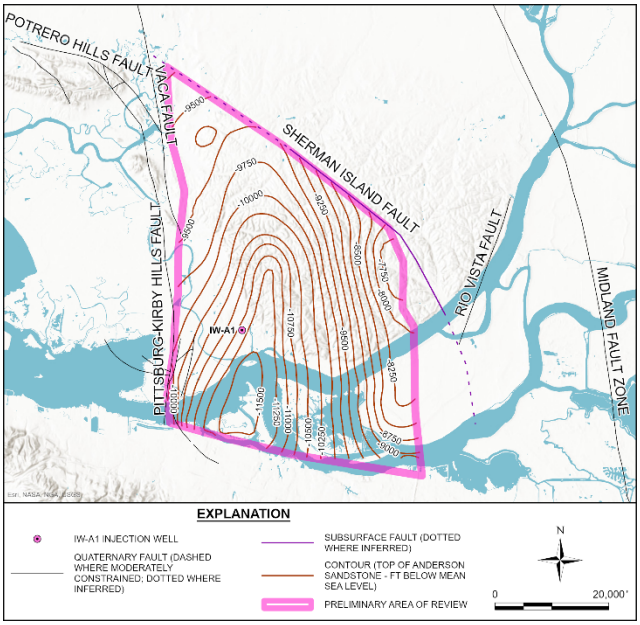

FIGURE A.I-5H. AoR BOUNDARY AND STRUCTURAL CONTOURS – TOP OF LOWER MARTINEZ SHALE

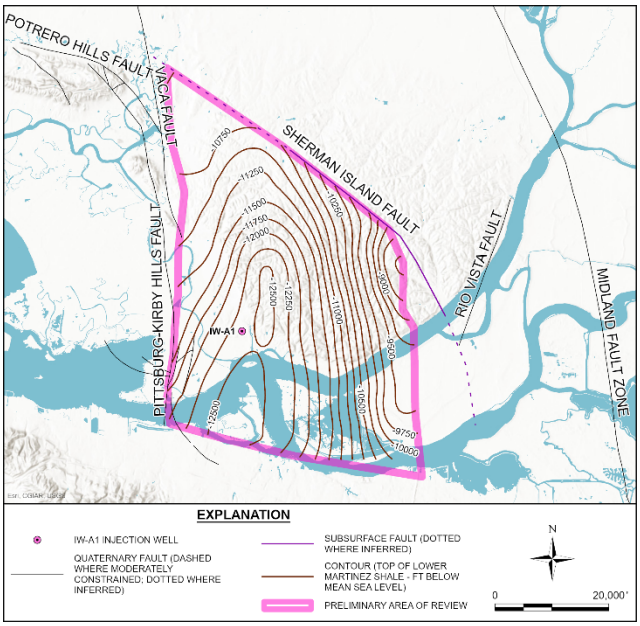

FIGURE A.I-5I. AoR BOUNDARY AND STRUCTURAL CONTOURS – BASE OF LOWER MARTINEZ SHALE

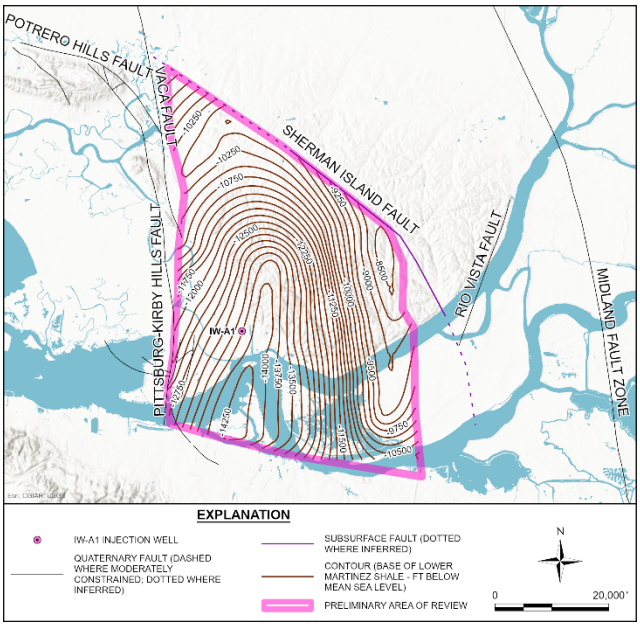

FIGURE A.I-5J. AoR BOUNDARY AND STRUCTURAL CONTOURS – ISOPACH OF NORTONVILLE SHALE

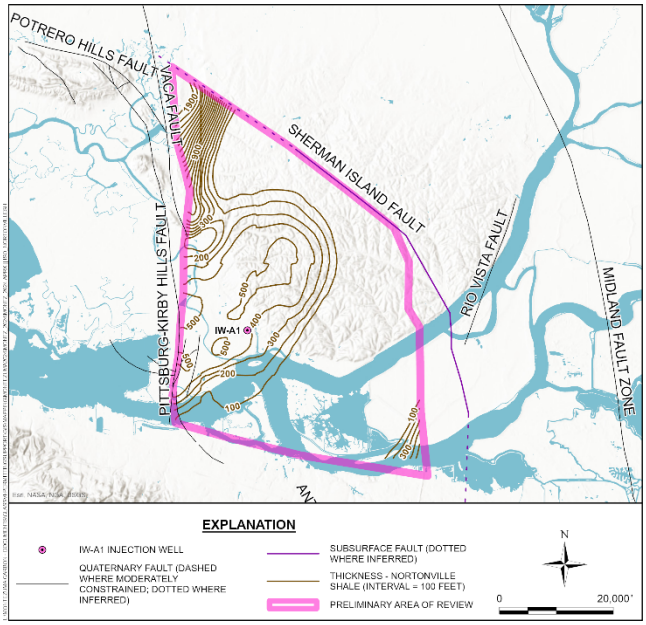

FIGURE A.I-5K. AoR BOUNDARY AND STRUCTURAL CONTOURS – ISOPACH OF DOMENGINE SANDSTONE

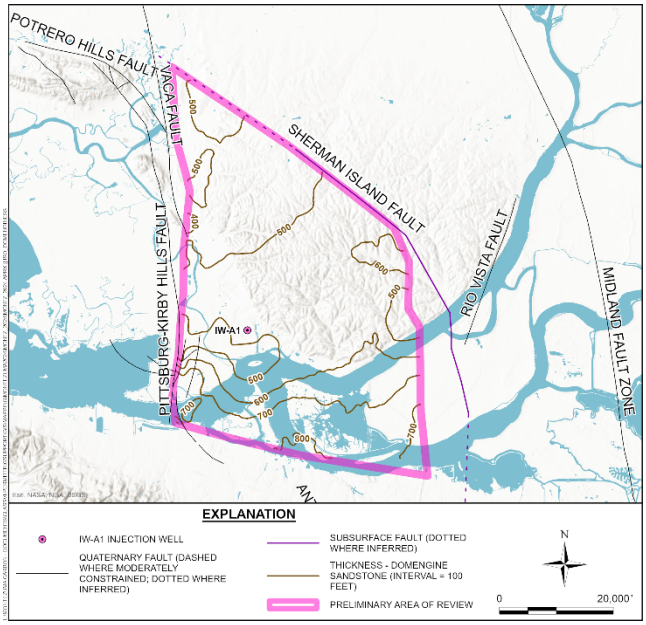

FIGURE A.I-5L. AoR BOUNDARY AND STRUCTURAL CONTOURS – ISOPACH OF CAPAY SHALE

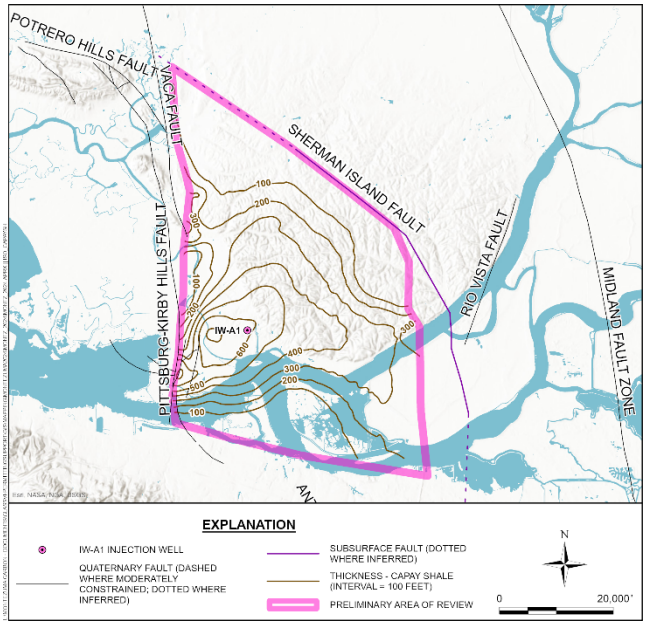

FIGURE A.I-5M. AoR BOUNDARY AND STRUCTURAL CONTOURS – ISOPACH OF HAMILTON SANDSTONE

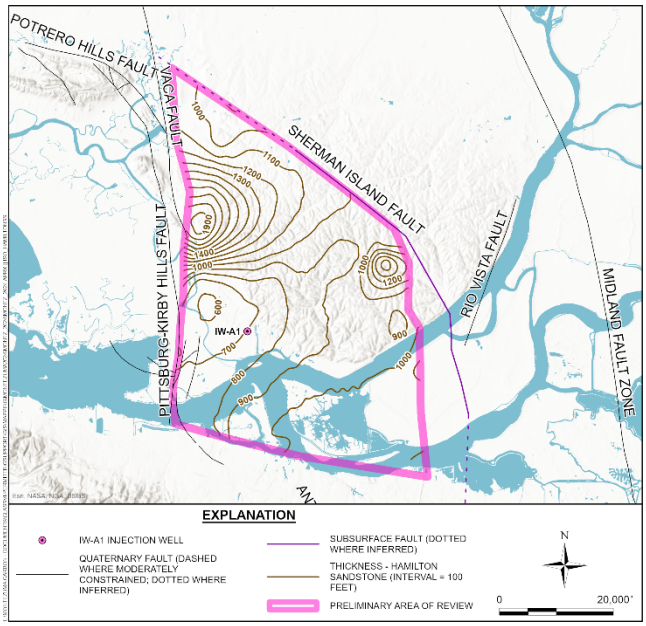

FIGURE A.I-5N. AoR BOUNDARY AND STRUCTURAL CONTOURS – ISOPACH OF MEGANOS SHALE

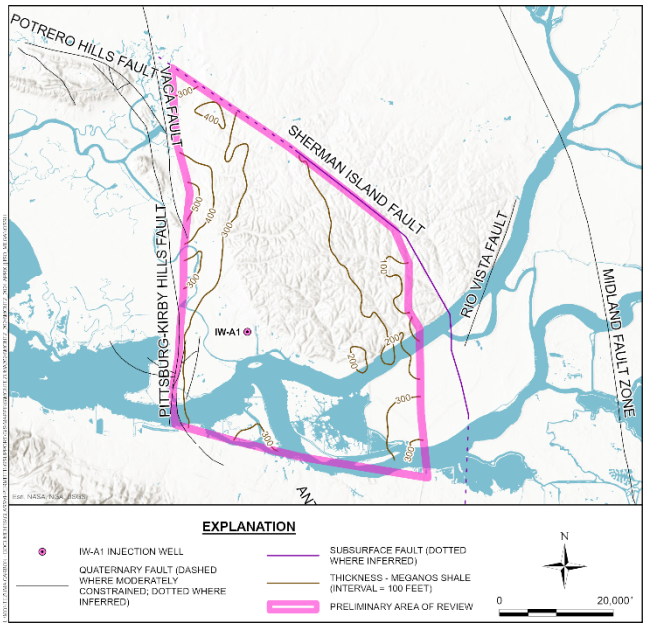

FIGURE A.I-5O. AoR BOUNDARY AND STRUCTURAL CONTOURS – ISOPACH OF UPPER MARTINEZ SHALE

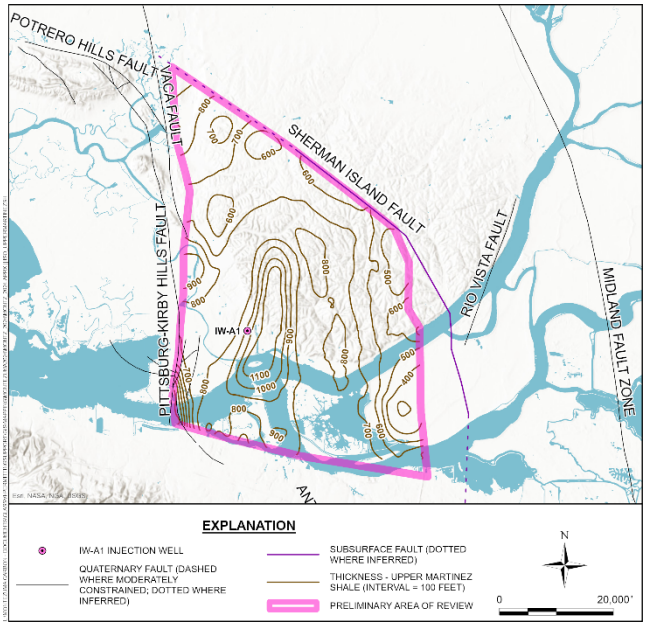

FIGURE A.I-5P. AoR BOUNDARY AND STRUCTURAL CONTOURS – ISOPACH OF ANDERSON SANDSTONE

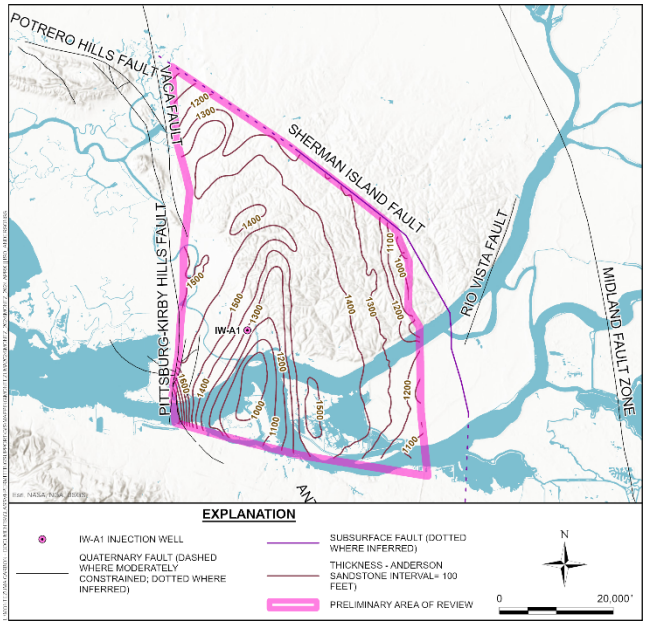

FIGURE A.I-5Q. AoR BOUNDARY AND STRUCTURAL CONTOURS – ISOPACH OF LOWER MARTINEZ SHALE

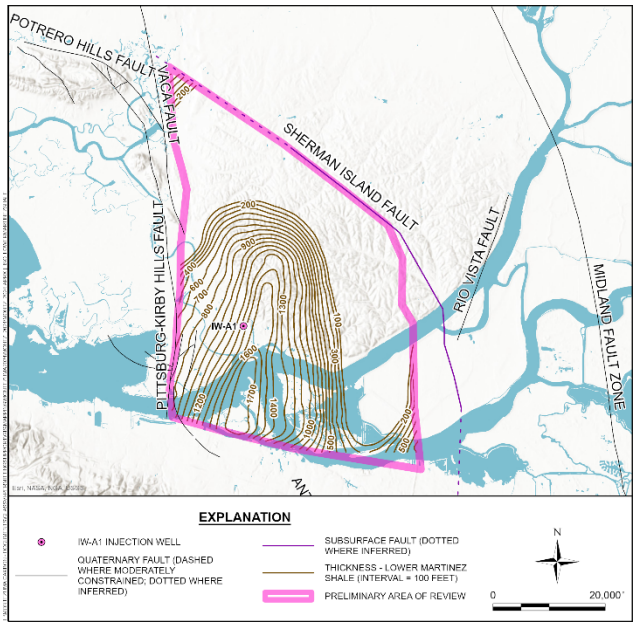

Holocene-Pleistocene-Pliocene [0-2,000 ft subsea]: For the most part, undifferentiated non-marine. Medium to dark gray-green sands, poorly consolidated, volcanic fragments, inclusive of the Tehama Formation. Interbedded soft, silty, massive gray-green and brown clays. Though there is typically a thin zone of very recent materials at and near the surface, a large portion of the lower section from this interval of rock has been named the Tehama Formation. The lowermost USDW zone in the MC project area is considered to occur within this unit at an approximate depth of 1,000-2,000 ft subsea (all subsequent depths are registered to sea level and ground level is less than 30 ft above sea level at IW-A1).

Upper Eocene [2000-7850 ft subsea]: Includes the Markley Sand, a fine to medium grained sand of gray-brown color interbedded with carbonaceous brown shales and the Sidney Flat Shale, a massive brown shale. This interval is anticipated to include about 80% shale.

Nortonville Shale [Confining unit] - middle Eocene [7,850-8,150 ft subsea]: Medium to dark gray-brown brittle shale, locally calcareous, with many fossils (forams and diatoms) (Johnson, 1992). This confinement zone is present throughout the study area (MacKevett 1992). This unit is shown as being hundreds of feet thick in all of the gas fields around the area, including Van Sickle and Suisun Bay fields to the west, Sherman Island and Rio Vista to the east, and Kirby Hill to the north. Site-specific data will be obtained for the upper and lower confining zones as part of the Pre-Operational Testing Program for the planned stratigraphic test well.

Domengine Sandstone [Potential future injection zone] - middle Eocene [8,150 -8,550 ft subsea]: This sand unit is one of the most productive zones in the area. An unconformity that eroded the Anderson and Hamilton sands to the west of the Kirby Hills fault lies at the base of this unit. This formation consists of very fine-medium grained, greenish-gray or white quartz sand, friable, moderately sorted, silty, glauconitic, shell fragments. Fining upwards sequences with two distinct sand units are separated by a more shaley section. Thus, this 400 ft interval is expected to have approximately 270 ft of net permeable zones. This zone is currently understood to have a similar capillary pressure fitting term λ (0.400) as the Hamilton Sandstone and Anderson Sandstone values used in the computational modeling (see the Area of Review and Corrective Action Plan document). Average sand porosity: 20%, range: 16-32%, average sand permeability 40mD, range: 10-100+mD. Thickness of >20 mD sands: 320 +-64 ft. Average total dissolved solids (TDS): 11,000 ppm, range: 10,200-13,000 ppm.

Capay Shale [Confining unit] – lower Eocene [8,550-9,200 ft subsea]: This shale unit is present in most of the project area. However, it is absent in an area along the west side of the Kirby Hill fault zone having been eroded. In the vicinity of planned injection, the thickness of the Capay Shale is currently understood to be 650 ft (i.e., 8,550 to 9,200 ft). This unit is composed of light-medium pure gray shale, soft-firm, gummy, moderately cohesive, with very-fine, sub-rounded clear quartz, moderate sorting, with abundant glauconite at the base (Johnson, 1992). As described in the Area of Review and Corrective Action Plan document, computational modeling of future CO_2 plume and pressure evolution during and following injection used literature-based parameters for the Capay shale. The values included 0.01 mD for horizontal permeability, 0.001 mD for vertical permeability, 0.20 for porosity, and a 0.412 for the capillary pressure fitting term λ. The current capillary pressure for supercritical CO_2 versus water is understood to be zero (i.e., negligible separate phase CO_2 within the unit). Site-specific data will be obtained for the upper and lower confining zones as part of the Pre-Operational Testing Program for the planned stratigraphic test well.

Hamilton Sandstone [Potential future injection zone] - lower Eocene [9,200-9,900 ft subsea]: This unit is actually found at the bottom of the Capay Formation, below the Capay Shale. It is described as a light gray, very fine-fine grained, micaceous, carbonaceous sand, friable, clear quartz (Ditzler, 1972). This 700 ft thick interval is estimated to have a net thickness of between 200 to 280 ft at the MC project site. The Hamilton Sand itself has a distinctive shape on the electric logs, with a predominantly shaley and silty sand character near the top gradually becoming more sandy and becoming much more permeable and sandy at the bottom several hundred feet of the zone. Similar to the Capay Shale, this unit is present across most of the project area, however is absent in an area along the west side of the Kirby Hill fault. In addition, beyond the Sherman Island fault, outside of the AoR and near the Midland Fault, there is minimal separation between the Hamilton Sandstone and the Anderson Sandstone (see Figure A.I-2). Average sand porosity: 18%, range: 14-26%,

average sand permeability 30mD, range: 10-50md. Thickness of >15 mD sands: 240 +-48 ft. Average total dissolved solids (TDS): 12,000, range: 10,500-13,000 ppm. (State of California, Division of Oil and Gas, Volume 3: Northern California Oil and Gas Fields). As described in the Area of Review and Corrective Action Plan document, computational modeling of future CO_2 plume and pressure evolution during and following injection used literature-based parameters for the Hamilton sandstone. The values included 250 mD for horizontal permeability, 50 mD for vertical permeability, 0.19 for porosity, and a 0.400 for the capillary pressure fitting term λ. The current capillary pressure for supercritical CO_2 versus water is understood to be zero (i.e., negligible separate phase CO_2 within the unit).

Meganos/Upper Martinez Shale [Confining unit] - lower Eocene [9,900-11,300 ft subsea]: Electric logs of the wells closest to the proposed drill site show that there is a thick continuous shale section below the Hamilton Sand that includes the Meganos Shale and the Upper Martinez Shale. The lower Eocene Meganos shale and the upper Paleocene Upper Martinez shales combine to form a thick confinement zone that is present in the entire project area east of the Kirby Hill fault. The base of the Meganos shale is an erosional unconformity and consists of light-medium, gray to black shale, soft, clayey. The Upper Martinez is a medium-dark brown, firm, hard siltstone, occasionally massive with light-medium gray claystone MacKevett (1992). The total thickness of the Meganos Shale and Upper Martinez Shale formations is expected to be 1,400 ft at the MC project site. As described in the Area of Review and Corrective Action Plan document, computational modeling of future CO_2 plume and pressure evolution during and following injection used literature-based parameters for the Meganos shale. The values included 0.01 mD for horizontal permeability, 0.001 mD for vertical permeability, 0.20 for porosity, and a 0.412 for the capillary pressure fitting term λ. The current capillary pressure for supercritical CO_2 versus water is understood to be zero (i.e., negligible separate phase CO_2 within the unit). Site-specific data will be obtained for the upper and lower confining zones as part of the Pre-Operational Testing Program for the planned stratigraphic test well.

Anderson Sandstone [Targeted injection zone] - middle Paleocene [11,300-12,600 ft subsea]: This sandstone unit can be very thick based on well control and seismic data mapped by MacKevett (1992). However, the unit does thin rapidly to the east towards the Rio Vista gas field, where it ends up being missing due to erosion. But, in the heart of the regional syncline, there is a large area in which the sand is at least several hundred feet thick around the outer portion and up to roughly 2,000 ft thick in the center of the regional syncline. In general, the Anderson sandstone is described as a light gray, fine-medium grained, micaceous quartz sand. Logs suggest two main sand packages with a more shaley interval in between. This is the thickest potential injection zone beneath the MC project site, with an expected total thickness of approximately 1,300 ft (MacKevett, 1992) near IW-A1. Average sand porosity: 20%, range: 16-28%, average sand permeability 200mD, range: 20-400mD. Thickness of >50 mD sands: 910 +--182 ft. Average total dissolved

solids (TDS): 17,000, range: 13,000-25,000 ppm. (State of California, Division of Oil and Gas publication TR10, Volume 3: Northern California Oil and Gas Fields). As described in the Area of Review and Corrective Action Plan document, computational modeling of future CO_2 plume and pressure evolution during and following injection used literature-based parameters for the Anderson sandstone. The values included 20 mD and 200 mD for horizontal permeability (two cases modeled), 4 and 40 mD for vertical permeability (two cases modeled), 0.20 for porosity, and a 0.400 for the capillary pressure fitting term λ. The current capillary pressure for supercritical CO_2 versus water is understood to be zero (i.e., negligible separate phase CO_2 within the unit).

Lower Martinez Shale [Confining zone] - lower Paleocene [12,600-13,900 ft subsea]: This shale layer is the lower confinement zone beneath the Anderson sandstone. The description of this unit (Johnson, 1999) is similar to that for the Upper Martinez Shale: medium-dark brown, firm, hard, siltstone, occasionally massive with light-medium gray claystone. There is a base Martinez sand unit named the McCormick sand which is described as a very fine-medium grained, white, quarzitic sand, friable, sorted (Johnson, 1999). However, the thickness of the Lower Martinez Shale should provide suitable confinement for the targeted Anderson injection zone. As described in the Area of Review and Corrective Action Plan document, computational modeling of future CO_2 plume and pressure evolution during and following injection used literature-based parameters for the Lower Martinez shale. The values included 0.01 mD for horizontal permeability, 0.001 mD for vertical permeability, 0.15 for porosity, and a 0.400 for the capillary pressure fitting term λ. The current capillary pressure for supercritical CO_2 versus water is understood to be zero (i.e., negligible separate phase CO_2 within the unit). Site-specific data will be obtained for the upper and lower confining zones as part of the Pre-Operational Testing Program for the planned stratigraphic test well.

A.I.5 GEOMECHANICAL/FLUID PRESSURE INFORMATION [40 CFR 146.82(A)(3)(IV)]

Fractures
Based on

1. “Wells within the AoR that intersect the confining and injection zones
2. 2D Seismic data within the AoR
3. Mackevitt (1992)

there are no faults or fractures within the AoR. With future 3D seismic data it may be possible to identify smaller faults and fractures that cannot be identified from existing log and 2D seismic data.

Rock Ductility

The computational modeling described in the Area of Review / Corrective Action Plan portion of this permit application present estimates of geomechanical properties based on literature for the area. The values that characterize rock ductility are repeated here:

TABLE A.I-1. GEOMECHANICAL PROPERTIES (BULK, YOUNG, SHEAR MODULUS)

Unit	Bulk Modulus (GPa)	Young's Modulus (Gpa)	Shear Modulus (Gpa)
Capay sh	17.5	28.2	11.4
Hamilton ss	19.8	31.2	12.6
Meganos/Upper Martinez sh	21.2	35.6	14.6
Anderson ss	25.2	42.2	17.3
Lower Martinez sh	27.0	47.5	19.7

Rock Strength

The computational modeling described in the Area of Review / Corrective Action Plan portion of this permit application present estimates of geomechanical properties based on literature for the area. The values that characterize rock strength are repeated here:

TABLE A.I-2. GEOMECHANICAL PROPERTIES (ROCK TENSILE STRENGTH)

Unit	Tensile Strength (Mpa)
Capay sh	7.3
Hamilton ss	7.5
Meganos/Upper Martinez sh	7.8
Anderson ss	8.1
Lower Martinez sh	8.5

Stress

No stress measurements of the confining or reservoir formation have been performed in the area. An in-situ stress direction of N35E +-12 was obtained from deep earthquake focal mechanisms in the region and borehole breakouts in the Rio Vista field (Unruh, et al, 2019).

Formation Pressure

Estimates of pore pressure and ranges for each of the formations of interest were obtained from mud weights used from Rio Vista to Suisun Bay and are illustrated in Figure A.I-6. The data used to generate the figure are primarily the Anderson 1-5 well (API 09520430; Figure A-3A of the Project Narrative) within the AoR, with a

"low" and "high" value based on varied considerations of the mud weights. Mud weights were 72 pounds per cubic foot (lb/ft^3) from 1,500 to 2,900 ft bgs, 77 to 81 lb/ft^3 from 3,850 to 13,050 ft bgs, 86 to 95 lb/ft$_3$ from 13,200 to 13,540 ft bgs, and 104 to 105 lb/ft^3 from 13,625 to 14,160 ft bgs. The section is normally pressured up until 10,000 ft where pore pressures begin to increase more quickly. Nearby deep wells that penetrate the Anderson UMC "GP" #1-5 and "Anderson" #1-7 both have mud weights below 80 lb/ft^3 down to 11,000 to 12,000 ft bgs, so we are confident that the Anderson and formations above will be normally pressured. The Anderson injection interval is expected to have a formation pressure ranging from about 6,000 psi at the top to 6,600 psi at the bottom, the upper confining unit is expected to have formation pressures of 5,400 psi at the top and the lower confining unit is expected to have a formation pressure of 7,300 at the bottom. These pressures will be updated after the drilling of MW-A1.

FIGURE A.I-6. PORE PRESSURE ESTIMATES VERSUS DEPTH

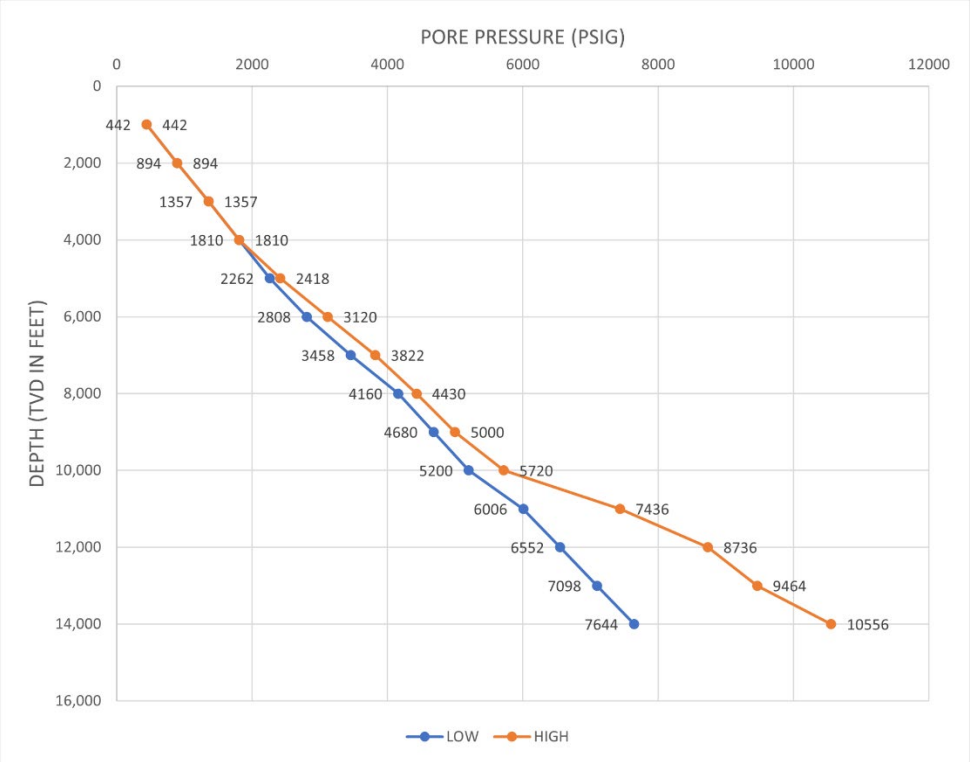

The Area of Review and Corrective Action Plan also presents regional information on the geomechanical and petrophysical properties of the study area. This regional information was used to develop the preliminary modeling and the AoR estimate. The Pre-operational Testing Program describes the plan for obtaining site-specific data on geomechanics and petrophysics of the area. This will include open hole logging as well as rock coring and analysis.

A.I.6 SEISMIC HISTORY [40 CFR 146.82(A)(3)(V)] AND POTENTIAL FOR INDUCED SEISMICITY

A.I.6.1 EARTHQUAKE HISTORY OF MONTEZUMA REGION AND FAULTING

Kirby Hills Fault

The Kirby Hills fault is an active fault that has a history of extremely deep earthquakes in the Montezuma area. Figure A.I-7A is a map showing event locations near the Kirby Hills fault for the period from 1969 and to 2019 (Klotsko, et al, 2023). As shown in the maps, nearly all earthquakes have M<3.0 with hypocenters at depths below 15 km, at least 7 km below the estimated top of basement. The focal mechanisms indicate predominantly right-lateral strike-slip motion. Some, but probably not all the seismicity within the seismic zone are associated with the Kirby Hills fault, although the majority of earthquakes are > 20 km, much deeper than most earthquakes within the San Andreas fault system. This raises the question whether this deep seismicity is actually related to the shallow Pitttsburg-Kirby fault zone. Other investigators have suggested that the Midland fault, which dips west, may be involved.

FIGURE A.I-7A. SEISMICITY HISTORY OF KIRBY HILLS FAULT AREA (1969 - 2014)

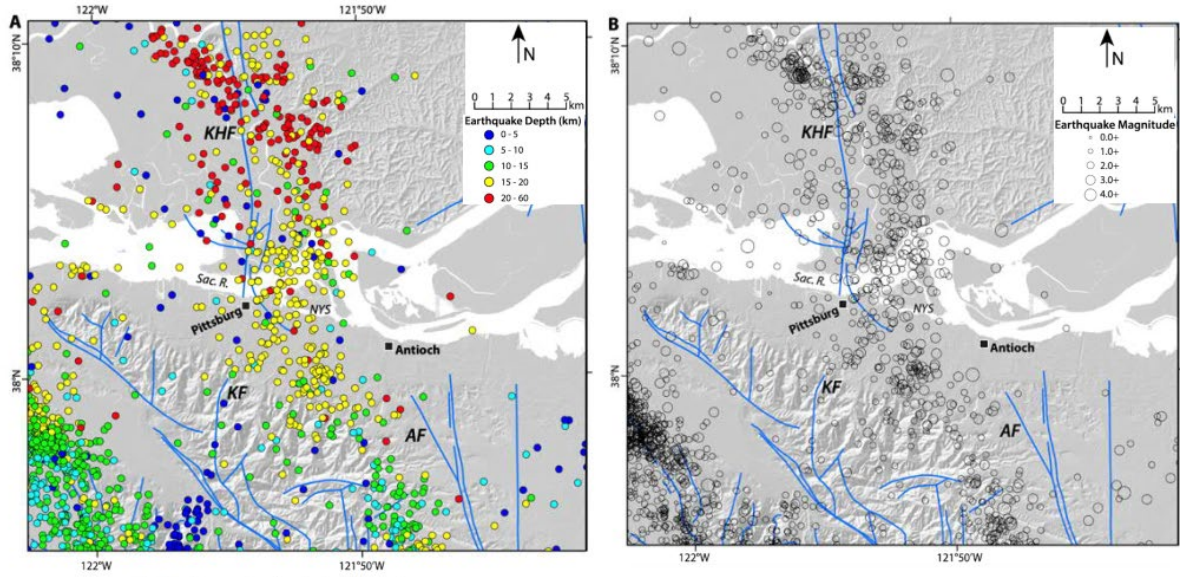

(A) Earthquake depth in kilometers (B) Earthquake magnitude

KHF - Kirby Hills Fault; KF Kirker Fault; AF Antioch Fault; Sac. R. - Sacramento River; NYS New York Slough

USGS and CGS, 2020; Horton et al., 2017

FIGURE A.I-7B. SEISMICITY HISTORY FOR STUDY AREA FROM 1969 TO END OF 2022

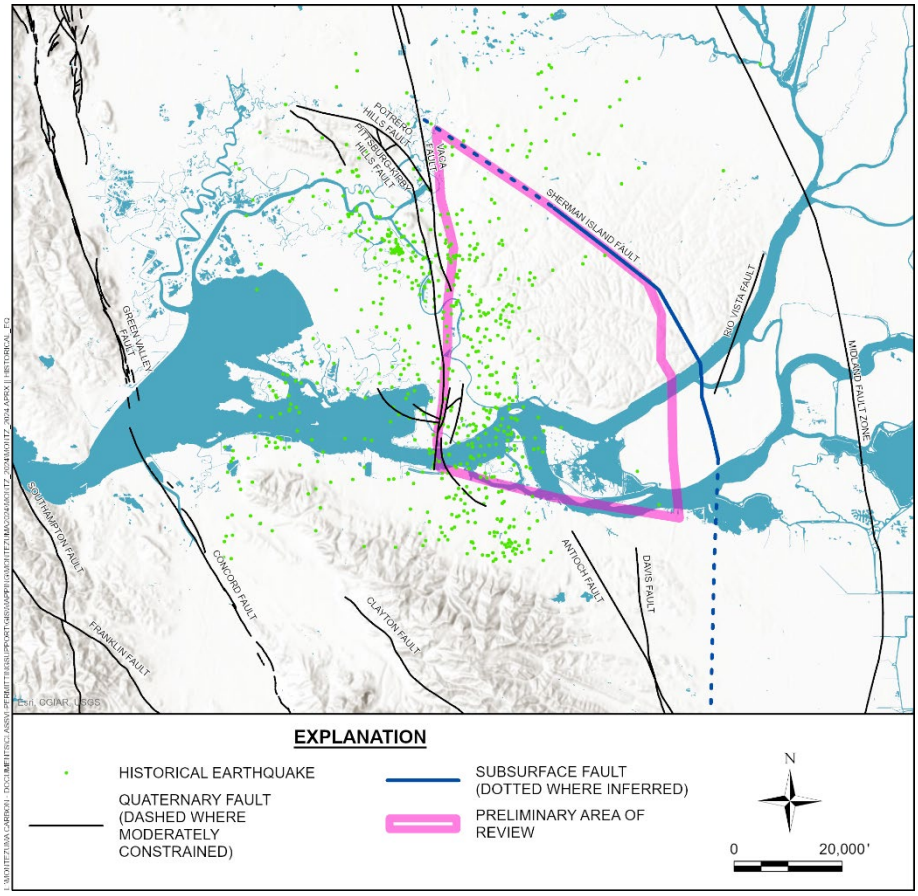

The source of Figure A.I-7B is an April 24, 2024 download from the USGS Advanced National Seismic System (ANSS) Comprehensive Earthquake Catalog (ComCat). The data are summarized in Appendix A.I-A.

The only large earthquake observed in the area was an (M~6) near Antioch in 1889. It is unknown where the hypocenter was located or even if it was on the Kirby Hills fault.

The Kirby Hills fault strikes roughly N/S and based on the deep hypocenters is assumed to dip about 75 degrees E. In the sedimentary section, the fault zone expands into numerous faults believed to be a flower structure (MacKevett,1992). At the surface the fault zone is about 0.5 km wide and there is evidence of Holocene deformation.

Sherman Island Fault

As shown in Figure A.I-7, the Sherman Island fault is inactive as it terminates near the Neogene boundary.

A.I.6.2 INDUCED SEISMICITY

Induced Earthquakes from Pressure Diffusion

Elevated pore pressures that travel from injection wells to a critically stressed fault via pressure diffusion can initiate slip by reducing the effective pressure, weakening the fault (Walsh and Zoback, 2015). Over the past 15 years in Oklahoma, high volume water disposal wells have induced large (M>5.0) earthquakes in basement rocks, often miles away from large volume injection wells. Wastewater is injected in the Arbuckle aquifer (which sits on top of basement) resulting in pressure perturbations that diffuse out into the aquifer and then down vertical faults into the basement. Prior to 2009, Oklahoma operators injected water at much lower rates and pressures and there were few induced earthquakes of a detectable magnitude. Beginning around 2009, large scale fracking and horizontal wells generated much larger volumes of wastewater and induced earthquakes increased in frequency. After the Pawnee M=5.8 earthquake the State of Oklahoma directed injection well operators to stop injection if an earthquake of M=4 or greater occurred within 6 miles of an injection well, and to reduce injection volumes if that earthquake occurred between 6 and 10 miles of the injection well. Earthquake magnitudes and frequencies dropped precipitously after the directive began in 2016-2017.

Small Induced earthquakes (M<2, White and Foxall, 2016) related to CO_2 injection have been created by a similar mechanism. The seismic networks monitoring the demonstration CCS project near Decatur, Illinois, recorded about 10,000 events in the magnitude range -2 to 1 from 2011 to 2014 when injection volumes were ~1 MMtonnes/year. Like the Arbuckle injection zone in Oklahoma, the Mt. Simon injection zone in Illinois sits on top of faulted basement and the induced seismicity mechanism is believed to be similar. When the injection zone was moved up away from the basement, induced earthquakes were reduced. A similar pattern of injection zone proximity to basement and frequency of induced earthquakes was observed in Oklahoma.

Induced earthquakes from a Poro-elastic Mechanism

Earthquakes have also been induced from pressure *reduction* due to oil and gas production (Segall, 1989, Sukale 2009). Given that negative fluid pressure changes should *increase* stress and make faults stronger, another mechanism for induced earthquakes called poro-elastic stress transfer was proposed in these papers. In poro-elastic stress transfer, the increased pressure caused by the injection zone radiates a poro-elastic response in the formation in all directions and travels farther and more rapidly than fluid pressure, which stays within the reservoir if there are confining layers above and below. Poro-elastic stress travels with velocities that are a small fraction (<1%) of elastic wave velocities, so the poro-elastic waves reach the hypocenter within minutes to hours depending on the distance between the pressure perturbation and the hypocenter. Unlike pressure diffusion, impermeable layers do not completely impede stress transfer.

An example of what are believed to be poro-elastic stress induced earthquakes due to wastewater injection is shown in Zhai, et al. (2021). The Delaware Basin of West Texas has experienced an increase in earthquake activity that has produced several M>5.0 earthquakes within the last three years. The Delaware Basin has also seen an increase in water disposal volumes in recent years. However, unlike Oklahoma, the injection zone is far above the basement, and there are permeability barriers between the injection zone and the earthquake hypocenter depths. Consequently, pressure diffusion is unlikely to be the mechanism for inducing deep seismicity here.

Preliminary Assessment of CCS Induced Seismicity Potential at Montenzuma Hills Site

The Montezuma site is quite different from the examples above.

1. The Montezuma injection interval is 2-3 miles above top of crystalline basement, and 8-12 miles above seismicity in the area.
2. The confining units are impermeable thick, continuous shales with an additional 2-3 miles of largely shale confining zones separating the reservoir from the basement.
3. All the major faults in the area (Kirby Hills, Midland, and Sherman Island) are known from gas production adjacent to the fault to be impermeable.
4. None of the huge volumes of gas withdrawn in the area (over 4 TCF) has affected pressures away from the fields nor was any induced seismicity or change in active seismicity due to gas production been observed indicating that poroelastic effects are insufficient for creating seismicity either in the reservoir or the basement.

Consequently, the risk of CO_2 injection causing large (M>4.5) events is negligible and if any seismicity is detected it is most likely to be unfelt small events near the reservoir interval and the injection well.

Small faults and fractures below the resolving power of 3D seismic data (25-50 ft of throw) cannot be ruled out in the AoR and could slip due to pressure changes in the reservoir, or changes in rock properties due to the plume. However, these earthquakes are highly unlikely to cause any damage.

Potential for Damage to Injection Wells or Compromise of Seals from Natural or Induced Seismicity

The report of Pratt, et al. (1978), concludes that there are virtually no examples of underground damage from the vibrations produced by earthquakes of any magnitude. Even the 1964 Alaska quake had no damage to underground structures including oil and gas wells in Cook Inlet. The report also states that underground examples of well damage are invariably correlated with fault displacement. In the Montezuma AoR, any fault

slip in the plume region (if there are any faults at all), will be far less than the thicknesses of the bounding shales and the seals will not be compromised. Even a small fault intersecting the well is highly unlikely, particularly because the well will be sited using 3D seismic data. Should one be encountered during drilling, the well will be sidetracked to avoid the fault. Based on the information reviewed by Pratt et al. (1978) and the absence of large faults within the AoR, there is minimal identified seismic risk to artificial penetrations, especially those that penetrate to consolidated materials.

A.I.7 HYDROLOGIC AND HYDROGEOLOGIC INFORMATION [40 CFR 146.82(A)(3)(VI), 146.82(A)(5)]

The Montezuma Hills are low-lying, reaching a maximum elevation of less than 90 meters (300 ft) above sea level. The hills drain predominantly to the Sacramento River to the southeast. The only perennial streams in the hills occupy some of these drainages. Minor seasonal streams drain the margins of the hills to the north and west. The water table depth in the Montezuma Hills may increase to as much as 30 m (100 ft) beneath the highest ridges (elevation 90 m [300 ft]) in the central portion of the hills, however, there are perennially wet drainages in this central area at an elevation of approximately 60 m (200 ft).

Groundwater assessment at the Montezuma Wetlands has identified multiple potential USDW zones, listed on Table A.I-3.

TABLE A.I-3. SHALLOW GROUNDWATER ZONES

Depth interval; thickness	Lithology	Notes
5-55 ft bgs; 50 ft	Clays, silts, and sands	Hydraulically connected to the Sacramento-San Joaquin River Delta. Considered a brackish aquifer by the Regional Water Board and not considered to be a source of drinking water
70-83 ft bgs; 13 ft	Sand	Hydraulically separated from the shallower aquifer
~1,000 to 3,000 ft bgs; 2,000 ft	Sandstone, siltstone, shale, and conglomerate	Lowermost USDW in the area

As shown on Figure A.I-8, the Montezuma Wetlands and Montezuma Hills are at the edge of the San Francisco and Sacramento River hydrologic regions for shallow groundwater.

FIGURE A.I-8. SHALLOW GROUNDWATER HYDROLOGIC REGIONS FOR AREA

The source for Figure A.I-8 is CDWR (2021). The site is north of the Antioch dote on the map.

The water table or alluvial aquifer is understood to regionally flow toward the Sacramento River (Figure A.I-9). In the vicinity of the site and near the river, the groundwater is in hydraulic communication with the river, and the flow direction may vary depending on river elevation.

FIGURE A.I-9. POTENTIOMETRIC SURFACE MAP FOR SACRAMENTO RIVER HYDROLOGIC REGION (WATER TABLE AQUIFER)

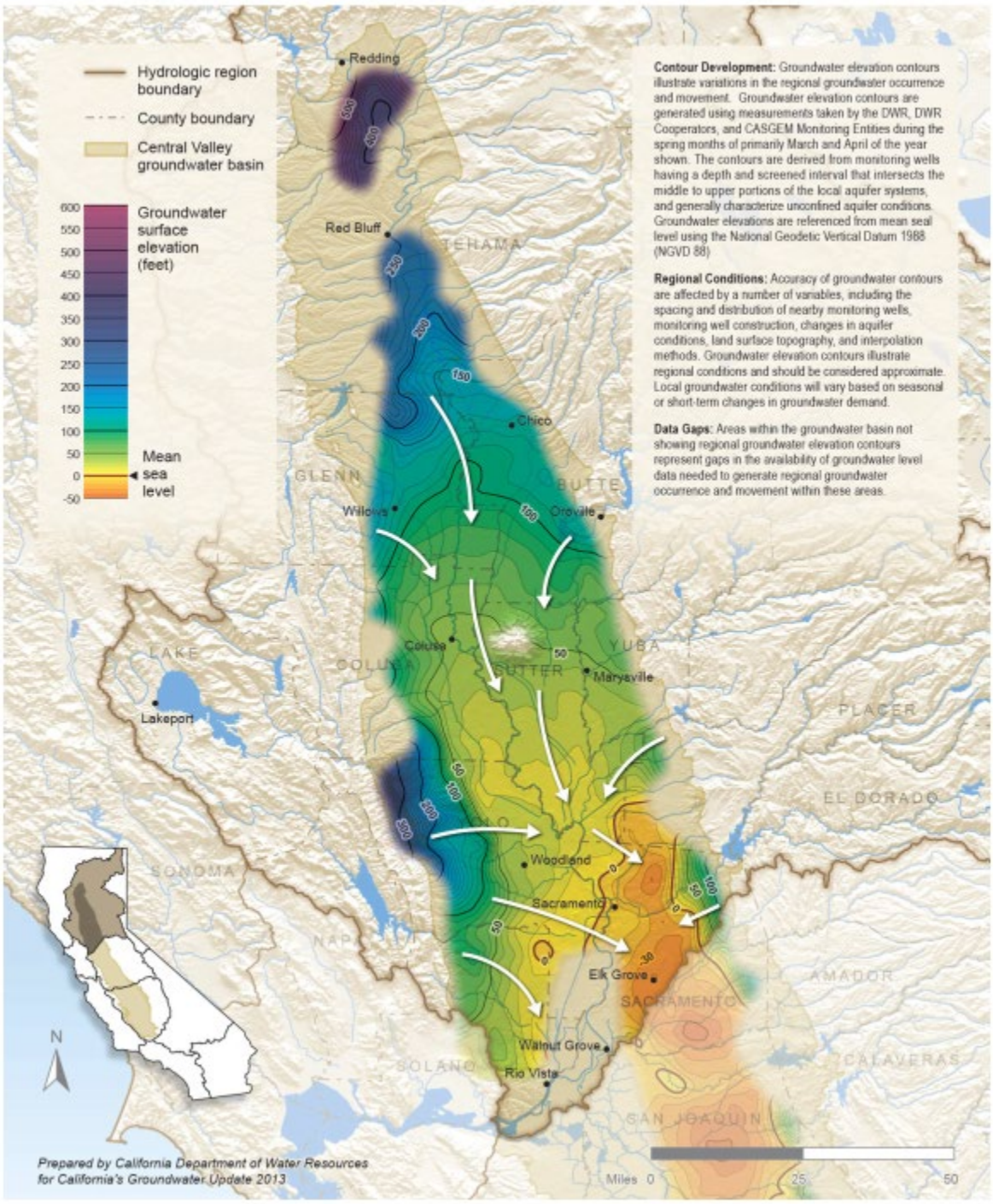

The source for Figure A.I-9 is CDWR (2015).

The maximum horizontal gradient occurs from the center to the edge of the Montezuma Hills, a minimum distance of 6.5 km (4 mi). Assuming the water table elevation to be 60 m (200 ft) at the center and sea level at the edge, this yields a gradient of about 0.01. Gradients outside this area can be expected to be much less due to the flat topography and pervasiveness of perennial water channels.

The average hydraulic conductivity in the Sacramento Valley aquifer is 0.9 m d^{-1} (3 ft d^{-1}) (Williamson et al., 1989). Combining this with the maximum gradient of 0.01 and an estimated effective porosity of 25% yields an estimated maximum linear groundwater velocity of 15 m yr^{-1} (50 ft yr^{-1}). While the hydraulic conductivities may be higher or lower, they are probably similar to the Sacramento Valley average. Water pressures are hydrostatic from the water table down to the Cretaceous Delta Shale.

Much of the site is located within the San Francisco Bay hydrologic region. As shown on Figure A.I-10, the site (north of Pittsburg on the map) is categorized as “low” for basin prioritization.

FIGURE A.I-10. GROUNDWATER BASIN PRIORITIZATION FOR PORTIONS OF SAN FRANCISCO BAY HYDROLOGIC REGION

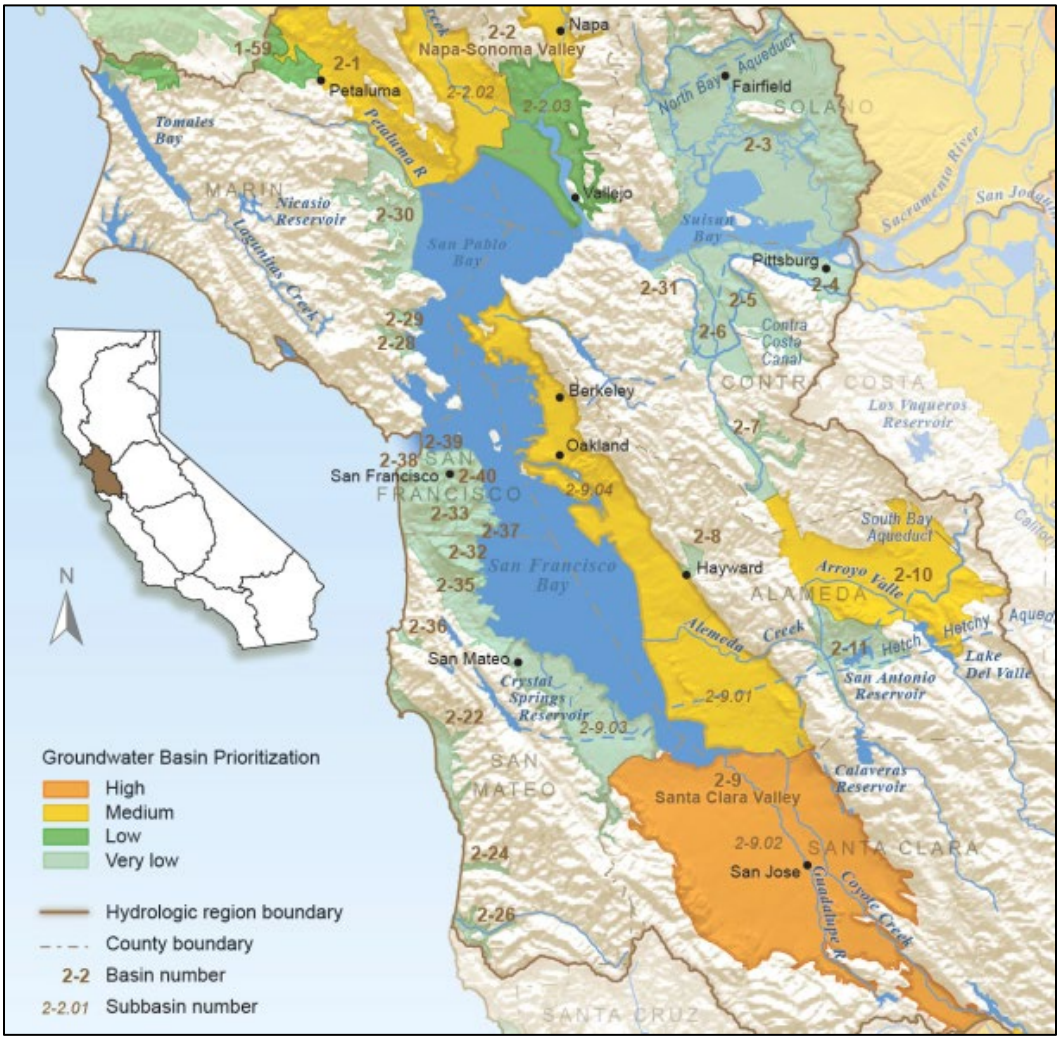

The source of Figure A.I-10 is CDWR (2015). The project area is north of the Pittsburg dot on the map.

The currently understood lowermost USDW in the area is the thick gravel-rich Tehama Formation, which is an approximately 610 m (2000 ft) thick aquifer that extends to about 915 m (3000 ft) below the surface. The Tehama Formation is a sedimentary rock unit that is primarily composed of sandstone, siltstone, shale, and conglomerate. It is part of the larger Cenozoic sedimentary sequence within the Sacramento Basin. The deposition of the Tehama Formation began during the late Cretaceous period, approximately 80 to 70 million years ago, and continued into the early Tertiary period. It represents a time when the Sacramento Basin was submerged beneath a shallow marine environment.

The Tehama Formation consists of layers of marine and non-marine sediments that were deposited in various environments, including coastal plains, estuaries, and shallow marine environments. The deposition of sediments was influenced by factors such as sea-level changes, tectonic activity, and sediment supply from nearby mountain ranges. The sandstone and conglomerate layers within the Tehama Formation indicate the presence of ancient river systems that transported and deposited coarse sediments. These sediments likely originated from the uplifted Sierra Nevada Mountains and other nearby sources. The siltstone and shale layers, on the other hand, represent finer-grained deposits that settled in calm marine or estuarine environments. The Tehama Formation is present widely across the Sacramento Valley east of the site, including as outcrops. As shown on Figure A.I-11, the Tehama formation has been identified more locally in Solano County north of the Sacramento River and has been reported as present as a surface expression in the Kirby Hill Fault Zone at Kirby Hill (MacKevett 1992).

FIGURE A.I-11. SOLANO COUNTY, CALIFORNIA GENERALIZED CROSS-SECTION, GROUND SURFACE THROUGH TERTIARY SEDIMENTS

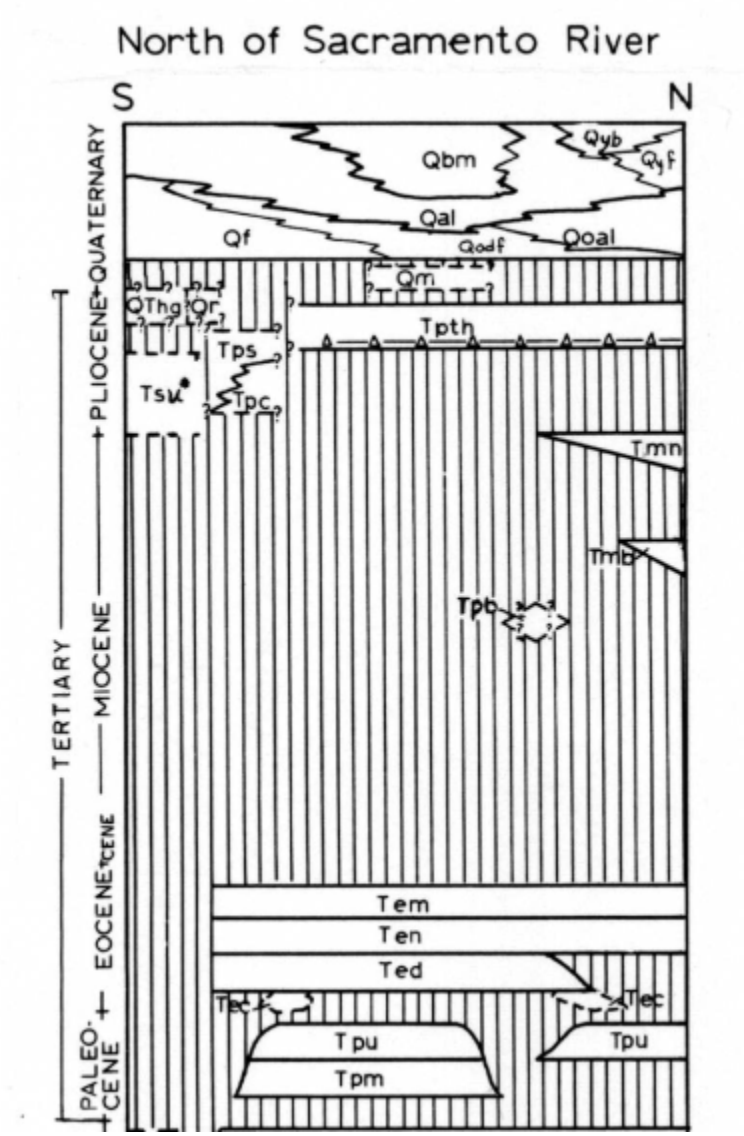

The source for Figure A.I-11 is Sims et al. (1973). Formations with "Q" designation are Quaternary and formations with "T" designation are Tertiary. The Tehama formation is designated as Tpth.

The Tehama Formation is an important groundwater resource for the Sacramento Valley east of the site, but this aquifer is not understood to be a drinking water resource in the project area. The town of Collinsville obtains drinking water from well CA4800511. This well has a screen interval of 240 to 300 ft bgs and is reported to be screened in the Wilcox aquifer, much shallower than the Tehama Formation. All water wells in the area listed as domestic or water supply in Appendix B-2 of the Area of Review and Corrective Action Plan

document (see Figure B-16 of that document for locations of those wells) have total depths less than 500 ft bgs, placing them within unconsolidated sediments above the Tehama Formation.

Oldenburg et al. (2010) compiled salinity data for deep groundwater near the Montezuma Hills. Those data, presented on Figure A.I-12, indicate a preponderance of values near or greater than 10,000 mg/L at depths greater than approximately 2,000 ft bgs. Salinity is only one component of TDS, so this also indicates that TDS values likely tend to be greater than 10,000 mg/L. However, the error bars for several formations, and some presented individual samples, are below the 10,000 mg/L threshold. This indicates the importance of groundwater assessment that will be conducted as part of the Pre-operational Testing program that is described in this permit application. That testing will be sufficient to characterize TDS values with depth within the project area, rather than in surrounding zones as depicted on Figure A.I-12.

FIGURE A.I-12. SALINITIES BY GEOLOGIC UNIT IN THE VICINITY OF THE PROJECT SITE

(From Oldenburg et al. 2003)

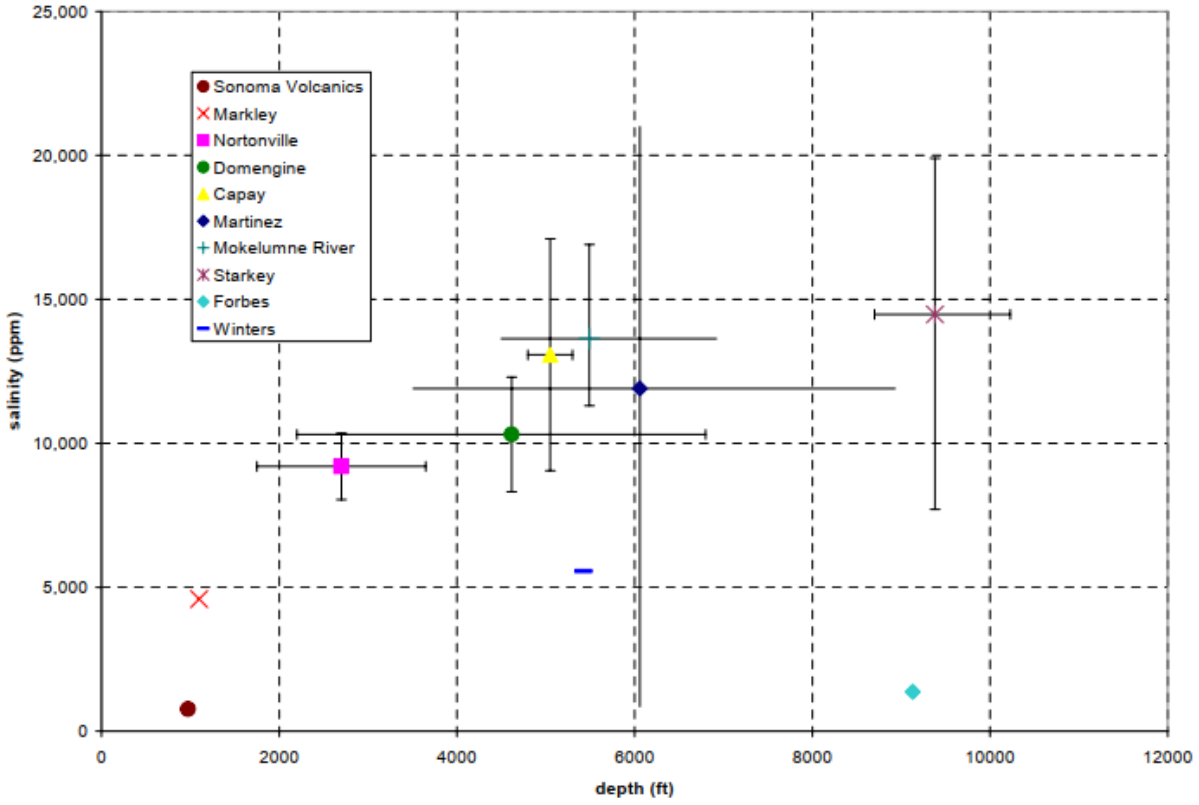

The Tehama Formation groundwater sis separated from the underlying deep saline formations by a thick, low permeability aquitard of clay-rich volcanoclastic sandstones. All CO_2 injection targets lie well below this aquitard and therefore there is good low permeable separation between the currently understood USDWs and the deep saline formations in the area.

A.I.8 GEOCHEMISTRY [40 CFR 146.82(A)(6)]

The amount of geochemical data available at present on the Montezuma Carbon Project is limited. Much of the lack of data is due to the rules of the State of California and how much of the data gained during the well drilling into the deep formations can be kept confidential and not released to the public. However, the testing & and monitoring efforts to be undertaken for this project will work to fill those data limitation, and much more will be known.

The Domengine zone is the only interval that has a geochemistry paper written about it. That paper is by Todd and Moore (1968), and it is entitled “Petrology of Domengine Formation (Eocene) at Potrero Hills and Rio

Vista, California" and was published in the Journal of Sedimentary Petrology. They describe the formation as a feldspathic subgraywacke unit that includes clayey sandstone, sandy siltstone, and silty shale. It accumulated under primarily transgressive marine conditions. This study was done from both outcrop samples in the Potrero Hills and from core samples in the Rio Vista gas field, located some 15 miles apart. Both of these areas are either in or near the MC project AoR. It was found that most of the Domengine is comprised of quartz, with 60%-70% being common quartz. The most common clay mineral was kaolinite. The most common rock fragments were metamorphics, which included quartz-muscovite schist, argillite, and aphanitic and plagioclase lath-bearing varieties. The average grain had subangular roundness and was between 0.09 and 0.19 mm in size.

A.I.9 SITE SUITABILITY [40 CFR 146.83]

The proposed injection site was previously studied for geologic suitability by Shell and LBNL as part of a DOE-supported pilot CO_2 injection project to handle the CO_2 from Shell's refinery in Martinez (Hymes, 2010). The pilot project proposed with drilling and formation property testing followed by injection and monitoring of a small amount of CO_2 into the Anderson sand. Based upon those previous efforts, Shell concluded that the site geology was very attractive, with the ability to safely store large volumes of CO_2. The reservoir zones were thick, porous, continuous sands and the relevant confining units are thick, laterally continuous shale units known to be flow and pressure barriers in nearby gas fields. However, at that time the economics for a carbon capture project of this potential scale were not justified. Those economics and governmental support have changed in recent years.

In the development of this proposal, we have built off the previous Shell/LBNL study, focusing it on our specific acreage in the Montezuma hills. We have performed additional studies of reservoir properties, incorporating not only well logs and seismic, but drilling and production data from nearby wells and gas fields and newer geologic studies of the area.

Using the geological, production, and geophysical information, we created a geologic and physical property model for plume and pressure front simulations which showed:

1. A single vertical well could inject one MMtonnes/year for over 40 years into the 1,300 ft thick Anderson sand reservoir located at 11,300 ft.
2. The plume extent is approximately 1.3 km in radius after 100 years and pressure increases of less than 1.7 MPa are created on the sealing faults to the east and west of the injection well. Evidence that the faults could be sealing include: a) presence of natural gas trapped against the Kirby Hills and Sherman Island faults, b) the "McDougal" well described above that intersected the Kirby Hills Fault found shales

adjacent to the Anderson Sandstone (MacKevett 1992), and c) a lattice of stratigraphic layer pinchouts and secondary faults associated with flower structures.

3. There is enough acreage at the site to put in at least three Anderson vertical injection wells on the current acreage. As described in the Area of Review and Corrective Action Plan computational modeling outputs, the CO_2 plume is far smaller than the AoR and is not predicted to approach the faults at these boundaries.
4. Other sand units (Domengine, Hamilton and potentially others), could potentially store comparable amounts of CO_2, and we believe that overall the site has a most likely storage estimate of over 250 MMtonnes of CO_2 at injectivity rates of over 5 MMtonnes per year.
5. Even if pessimistic forecasts of reservoir parameters are used, the site has storage potential of over 80 MMtones at rates of over 2 MMtonnes per year.

Risks of Leaks

There is a negligible risk of leakage into shallow units due to injection. First, the confining units are thick, continuous, clay-rich shales that extend in intervals for thousands of feet above the injection interval. Second, production data from nearby gas fields has demonstrated that the reservoirs are not in communication. Third, the major faults in the area (Kirby Hills, Midland, and Sherman Island) are known from gas production to be traps. Fourth, the plume only extends 1.3 km away from IW-A1 and there is no evidence of faulting near the injection well, and the shales above and below the reservoir are continuous far past the modeled plume extent.

A.I.10 REFERENCES

Burroughs, E., 1967, Rio Vista gas field: California Division of Oil and Gas, Summary of Operations: California Oil Fields, vol. 53, No. 2 – Part 2, p. 25-33.

California Department of Water Resources (CDWR). 2015. California's Groundwater Update 2013. Bulletin 118. April.

CDWR. 2020. California's Groundwater Update 2021. Bulletin 118.

California Division of Oil and Gas, 1982, California oil and gas fields, Northern California: Publication TR10, vol. 3. data sheets, pages of fields as follows: Denverton Creek, p. 74-75; Kirby Hill, p. 128-129; Kirby Hill North, p. 130-131; Potrero Hills, p. 220-221; Rio Vista, p. 236-239; Ryer Island, p. 249-250; Sherman Island, p. 261-262; Van Sickle Island, p. 303-304.

Cherven, V.B., 1983, Mesozoic through Paleogene evolution of the Sacramento basin, California, in Cherven, V.B. and Graham, S.A., eds., Geology and Sedimentology of the Southwestern Sacramento Basin and East Bay Hills: Field Trip Guidebook, Pacific Section, Society of Economic Paleontologists and Mineralogists, Los Angles, p. 21-31.

Crane, R.C., 1995, Geology of the Mt. Diablo region and East Bay hills, in Sangines, E.M., Andersen, D.E., and Buising, A.V., eds., Recent Geologic Studies in the San Francisco Bay Area: Pacific Section SEPM (Society for Sedimentary Geology), Volume 76, p. 87-114.

Ditzler, Clark C., 1972, Sherman Island Gas Field, in Selected Papers present to San Joaquin Geological Society, Volume 4, p. 21-25.

Division of Oil, Gas and Geothermal Resources (DOGGR), 1982a, California Oil and Gas Fields, Volume III – Northern California; Contour maps, cross sections and data sheets: California Department of Conservation, 330 p. (available from *http://repository.usgin.org/category/place-keywords/california*; last accessed 4/8/22)

Division of Oil, Gas, and Geothermal Resources (DOGGR) 1982b, Sherman Island gas field, in California Oil and Gas Fields, vol. III, Northern California: California Department of Conservation, Division of Oil and Gas, publication TR10.

Graham, S.A., Gavigan, C., McCloy, C., Hitzman, M., Ward, R., and Turner, R., 1983, Basin evolution during the change from convergent to transform continental margin: an example from the Neogene of California, in Cherven, V.B., and Graham, S.A., eds., Geology and Sedimentology of the Southwestern Sacramento Basin and East Bay Hills: Field Trip Guidebook, Pacific Section, Society of Economic Paleontologists and Mineralogists, Los Angles, p. 101-118.

Hector, Scott, 2000, Stratigraphic Variations in the Paleocene and Upper Cretaceous Sands and their effect on gas entrapment, Denverton Creek gas field, Sacramento Valley, (abstract), AAPG Search and Discovery Article #90911, Pacific Section and Western Region, Society of Petroleum Engineers, Long Beach, CA.

Hector, Scott, 2014, Lindsey Slough Gas Field: History of Development, (abstract), Pacific Section AAPG, SPE, and SEPM Technical Conference, Bakersfield, CA.

Hector, Scott, 2014, Rio Vista Gas Field: History of Development, (abstract), Pacific Section AAPG, SPE and SEPM Technical Conference, Bakersfield, CA.

Hymes, E., 2010, Northern California CO2 Reduction Project Final Scientific/Technical Report

Ingersoll, R. V., and Dickinson, W. R., 1981, Great Valley Group (sequence), Sacramento Valley, California, in Frizzell, V., ed., Upper Mesozoic Franciscan rocks and Great Valley sequence, central Coast ranges, California (Annual Meeting, Pacific Section SEPM field trips 1 and 4): Pacific Section, Society of Economic Paleontologists and Mineralogists, p. 1–33.

Johnson, D. S., 1992, Rio Vista Field, in Beaumont, Edward A. and Foster, Norman , compilers, Structural Traps III Tectonic Fold and Fault Traps: Treatise of Petroleum Geology: Atlas of Oil and Gas Fields, American Association of Petroleum Geologists, p. 243-264.

Johnson, D. S., 1990, Rio Vista gas field – USA, Sacramento Basin, Calif. in Foster, N. H., and Beaumont, E.A., eds., Atlas of oil and gas fields, Structural Traps III, AAPG. Treatise of Petroleum Geology, Atlas of Oil and Gas Fields, Tulsa, Oklahoma, U.S.A.

Klotsko, Shannon, Jillian Maloney, and Janet Watt. 2023, Shallow deformation on the Kirby Hills fault, Sacramento–San Joaquin Delta, California (USA), revealed from high-resolution seismic reflection data and coring in a fluvial system. *Geosphere*.

Krug, E.H., Cherven, V.B., Hatten, C.W., Roth, J.C., 1992, Subsurface structure in the Montezuma Hills, southwestern Sacramento basin, in Cherven, V.B., and Edmondson, W.F., eds., Structural Geology of the Sacramento Basin: Volume MP-41, Annual Meeting, Pacific Section, Society of Economic Paleontologists and Mineralogists, p. 41-60.

Lodi Gas Storage, LLC, 2007, Kirby Hill Phase II Natural Gas Storage Facility – Initial Study and Subsequent Mitigated Negative Declaration.

MacKevett, N.H., 1992, The Kirby Hills fault zone, in Cherven, V.B., and Edmondson, W.F., eds., Structural Geology of the Sacramento Basin: Volume MP-41, Annual Meeting, Pacific Section, Society of Economic Paleontologists and Mineralogists, p. 61-78.

Myer, L., L. Chiaramonte, T. M. Daley, D. Wilson, W. Foxall, J. H. Beyer, 2010, Potential for Induced Seismicity Related To The Northern California CO2 Reduction Project Pilot Test, Solano County, California , LLNL-TR-435831 June 15.

Oldenburg, Curtis M. and Preston D. Jordan, 2017, Long-Term Viability of Underground Natural Gas Storage in California An Independent Review of Scientific and Technical Information, California Council on Science and Technology December.

Oldenburg, C. M., Jordan, P., Mazzoldi, A., Wagoner, J., Bryant, S. L., and Nicot, J. 2010. Certification Framework, Leakage Risk Assessment for CO2 Injection at the Montezuma Hills Site, Solano County, California. May 26.

Pacific Section American Association of Petroleum Geologist, Geology of the Sacramento Basin, Publication No. MP-41, p. 41-60 and p. 61-78.

Pasquini, D.E., and Milligan, H.L., 1967, Correlation Section 15, Sacramento Valley, Suisun Bay to Lodi: Pacific Section, American Association of Petroleum Geologists.

Pepper, Miles W. and Johnson, Dane, 1992, The Midland Fault System, Southern Sacramento Basin, California, in Cherven, V.C., and Edmondson, W.F., eds., Structural Geology of the Sacramento Basin, Pacific Section, American Association of Petroleum Geologists, Publication No. MP-41, p. 27-40.

Pratt, H. R., W. A. Hustrulid, D. E. Stephenson, 1978, Earthquake Damage to Underground Facilities, Environmental Transport Division.

Segall, P., 1989, Earthquakes triggered by fluid extraction, Geology, 17, 942–946.Suckale, J. (2009), Induced seismicity in hydrocarbon fields, Adv. Geophys., 51, 55–106.

Sims, J. D., Fox Jr., K. F., Bartow, J. A., and Helley, E. J. 1973. Preliminary Geologic Map of Solano County and Parts of Napa, Contra Costa, Marin, and Yolo Counties, California.

Suckale, J. (2009), Induced seismicity in hydrocarbon fields, Adv. Geophys., 51, 55–106.

Sullivan, R., Sullivan, M.D., Dedmon, P., and Edwards, S.W., 2021a, The occurrence and mining of coal and sand deposits in the Middle Eocene Domengine Formation of the Mount Diablo Coalfield, California, in Sullivan, R., Sloan, D., Schwartz, D., and Unruh, J., Regional Geology of Mount Diablo, California: Its Tectonic Evolution on the North American Plate Boundary: Geological Society of America Memoir 217, p. 65-95.

Sullivan, R., Sullivan, M.D., Edwards, S.W., Sarna-Wojicicki, A., Hackworth, R.A., Deino, A.L., 2021b, The mid-Cenozoic succession on the northeast limb of Mount Diablo anticline, California-a stratigraphic record of tectonic events in the forearc basin, in Sullivan, R., Sloan, D., Schwartz, D., and Unruh, J., Regional Geology of Mount Diablo, California: Its Tectonic Evolution on the North American Plate Boundary: Geological Society of America Memoir 217, p. 269-303.

Todd, Thomas W. and William A. Monroe**,** 1968, Petrology of Domengine Formation (Eocene), at Potrero Hills and Rio Vista, California: Journal of Sedimentary Research, vol. 38, no. 4, p. 1024-1039.

Unruh, J., 2021, Upper plate deformation during blueschist exhumation, ancestral western California forearc basin, from stratigraphic and structural relationships at Mount Diablo and in the Rio Vista Basin, in Sullivan, R., Sloan, D., Schwartz, D., and Unruh, J., Regional Geology of Mount Diablo, California: Its Tectonic Evolution on the North American Plate Boundary: Geological Society of America Memoir 217, p. 179-200.

Unruh, J., Hitchcock, C., Blake, K., and Hector, S., 2016, Characterization of the Southern Midland Fault in the Sacramento-San Joaquin Delta, in Ferriz, H. and Anderson, R., eds., Applied Geology in California: Association of Engineering Geologists, Special Publication 26, p. 757-776.

Unruh, J.R., and Hector, S.T., 1999, Subsurface Characterization of the Potrero-Ryer Island Thrust System, Western Sacramento-San Joaquin Delta, Northern California: Final Technical Report submitted to the U.S. Geological Survey, National Earthquake Hazards Reduction Program award number 1434-HQ-96-GR-02724, 32 p.

Unruh, J, Wong, I, and Smith, S. (2015), Seismotectonic Characterization of the Coast Ranges-Sierran Block Boundary Zone, California FINAL TECHNICAL REPORT U. S. Geological Survey National Earthquake Hazards Reduction Program.

Walsh, F.R., and Zoback, M.D., 2015, Oklahoma's recent earthquakes and saltwater disposal: Science Advances, v. 1, e1500195, doi:10.1126 /sciadv.1500195.

White, J. A, and Foxall, W., 2016, Assessing induced seismicity risk at CO_2 storage projects: recent progress and remaining challenges. International Journal of Greenhouse Gas Control, vol. 49, p. 413-424. https://doi.org/10.1016/j.ijggc.2016.03.021

Williamson, A.K., Prudic, D. E., and Swain, L. A., 1989, Ground-water Flow in the Central Valley, California. U. S. Geological Survey Professional Paper 1401 -D.

Zhai, G., M. Shirzaei, and M. Manga (2021) Widespread deep seismicity in the Delaware Basin, Texas, is mainly driven by shallow wastewater injection, PNAS, vol. 118, e2102338118.

Zieglar, D. L., and J. H. Spotts, 1978, Reservoir and source-bed history of the Great Valley, California: American Association of Petroleum Geologists Bulletin, vo. 62, p. 813-826.

SECTION A.I. SITE CHARACTERIZATION
40 CFR 146.82(a)(2), (3), (5), and (6)

APPENDIX A.I-A

TABULATED SEISMICITY HISTORY FOR STUDY AREA FROM 1969 TO END OF 2022

APPENDIX A.I-A. TABULATED SEISMISCITY HISTORY FOR STUDY AREA FROM 1969 TO END OF 2022

Date/time	Latitude	Longitude	Depth (km)	Magnitude	Horizontal Error (km)	Depth Error (km)	Magnitude Error
2022-12-08T03:56:20.630Z	38.14417	-121.8105	16.49	1.44	0.8	0.8	0.185
2022-11-11T22:45:07.250Z	38.07733	-121.9996667	16.28	1.46	0.37	0.59	0.228
2022-11-09T11:45:28.630Z	38.11233	-121.9431667	19.29	1.45	0.59	0.91	0.153
2022-11-09T08:45:37.160Z	38.12683	-121.9393333	21.97	1.71	0.61	0.27	0.185
2022-11-09T08:03:26.080Z	38.11283	-121.9223333	22.1	2	0.4	0.3	0.164
2022-09-28T09:58:56.810Z	38.0705	-121.9991667	16.53	2.06	0.19	0.35	0.144
2022-09-21T10:16:31.480Z	38.19267	-122.0316667	-0.05	1.62	0.26	0.46	0.291
2022-09-02T18:41:59.150Z	38.06817	-122.0053333	14.68	1.72	0.37	0.71	0.25
2022-07-07T01:39:02.140Z	38.17617	-121.9991667	17.61	1.63	0.33	0.58	0.243
2022-06-02T18:44:17.200Z	38.08	-122.0098333	16.09	1.86	0.25	0.38	0.141
2022-06-02T13:25:33.540Z	38.08217	-122.0118333	16.73	1.77	0.26	0.38	0.232
2022-06-02T13:22:43.990Z	38.06983	-121.9995	15.91	1.98	0.2	0.25	0.146
2022-06-02T13:16:44.610Z	38.0775	-122.0081667	16.29	2.24	0.21	0.34	0.105
2022-06-02T13:14:30.070Z	38.073	-121.9986667	15.53	1.83	0.21	0.33	0.154
2022-06-02T12:42:04.570Z	38.069	-121.9931667	15.97	1.92	0.19	0.33	0.168
2022-06-02T12:14:21.330Z	38.07133	-121.9946667	15.88	1.71	0.21	0.32	0.222
2022-06-02T12:07:22.230Z	38.0765	-122.0076667	18.43	4.14	0.17	0.24	
2022-04-30T07:36:53.220Z	37.99983	-121.8806667	19.67	1.77	0.26	0.55	0.189
2022-02-07T03:25:08.040Z	38.06583	-121.922	21.15	1.75	0.29	0.44	0.282
2021-04-22T06:39:31.280Z	38.272	-121.861	23.35	1.88	0.28	0.27	0.284
2020-12-26T22:07:30.860Z	38.0335	-121.9726667	8.33	2.62	0.24	0.48	0.28
2020-12-25T07:53:44.380Z	38.044	-121.9811667	-0.12	1.6	0.41	0.5	0.188
2020-11-29T13:44:56.600Z	38.08983	-121.8943333	17.96	1.78	0.33	0.44	0.162
2020-11-18T04:33:09.970Z	38.09967	-121.8793333	20.32	2.03	0.34	0.29	0.216
2020-11-18T01:49:33.950Z	38.078	-121.8666667	17.98	2.02	0.3	0.4	0.2
2020-11-12T16:24:00.820Z	38.1385	-121.941	0.38	1.45	0.27	0.33	0.155
2020-06-01T01:32:27.290Z	38.02583	-121.8966667	18.51	1.87	0.26	0.39	0.291
2020-05-26T12:54:27.210Z	38.195	-121.9006667	25.16	2.26	0.35	0.39	0.165
2020-05-22T00:05:02.550Z	38.1255	-121.912	19.45	1.8	0.76	0.62	0.258
2020-04-27T19:09:25.280Z	38.01333	-121.8846667	17.47	1.55	0.48	0.93	0.306
2020-04-22T23:53:33.730Z	38.1615	-121.8468333	20.67	1.93	0.8	0.53	0.161
2020-04-22T23:48:09.710Z	38.16583	-121.8703333	22.96	2.05	0.42	0.32	0.251
2020-04-04T13:36:40.210Z	38.06333	-121.9058333	16.36	1.68	0.3	0.71	0.241
2020-04-04T10:02:44.000Z	38.05	-121.9095	17.88	2.43	0.25	0.42	0.231
2019-12-07T19:18:51.490Z	38.04383	-121.903	16.73	2.06	0.31	0.83	0.216
2019-10-21T03:11:21.630Z	38.068	-121.9131667	19.52	1.95	0.26	0.42	0.165
2019-09-21T00:01:22.090Z	38.03517	-121.9013333	18.33	1.57	0.43	0.69	0.086
2019-09-13T22:31:29.160Z	38.04317	-121.9063333	19.26	1.69	0.4	0.72	0.225
2019-09-07T09:31:06.010Z	38.2385	-121.774	25.71	1.95	0.55	1.18	0.253
2019-08-29T20:53:26.590Z	38.03767	-121.8531667	2.48	1.57	0.34	0.98	0.17
2019-08-10T20:12:53.600Z	38.10483	-121.8981667	20.49	1.99	0.33	0.25	0.145
2019-08-09T11:53:12.470Z	38.124	-121.9405	19.45	1.81	0.59	0.51	0.285
2019-06-10T07:34:21.730Z	38.09433	-121.989	17.74	1.57	0.3	0.6	0.177
2019-06-05T15:10:57.880Z	38.14733	-121.9445	4.57	1.37	0.63	1.34	0.09
2019-06-05T12:54:41.200Z	38.09367	-121.9878333	15.58	1.52	0.35	0.81	0.175
2019-05-28T05:53:52.860Z	38.2145	-121.7855	21.99	2.07	0.25	0.38	0.218
2019-04-28T16:50:47.750Z	38.0715	-121.895	4.03	1.14	0.51	1.2	0.155
2018-12-14T07:07:04.980Z	38.041	-121.9071667	19.1	2.43	0.31	0.35	0.161
2018-10-24T23:25:32.300Z	38.15467	-121.8645	21.9	1.98	0.46	31.61	0.231
2018-09-22T11:21:23.760Z	38.08867	-121.9416667	22.67	2.71	0.18	0.2	0.122
2018-08-27T16:09:43.520Z	38.11017	-121.9555	21.04	2.45	0.27	0.42	0.171
2018-08-05T14:35:51.000Z	38.18283	-121.9098333	24.07	2.89	0.34	0.25	0.169
2018-08-02T17:01:55.420Z	38.17717	-121.8693333	21.9	2.91	0.27	0.17	0.186
2018-08-02T12:12:47.740Z	38.19817	-121.9543333	21.1	2.18	0.18	0.33	0.164
2018-07-28T09:57:48.810Z	38.2015	-121.9498333	0.99	1.77	0.48	0.76	0.184

APPENDIX A.I-A. TABULATED SEISMISCITY HISTORY FOR STUDY AREA FROM 1969 TO END OF 2022

Date/time	Latitude	Longitude	Depth (km)	Magnitude	Horizontal Error (km)	Depth Error (km)	Magnitude Error
2018-07-17T16:47:51.910Z	38.05533	-121.9506667	19.75	1.95	0.48	0.2	0.214
2018-07-16T17:16:26.730Z	38.04867	-121.9776667	18.38	1.49	0.45	0.59	0.246
2018-06-08T00:41:00.080Z	38.09783	-121.8845	19.05	2.03	0.31	0.48	0.172
2018-05-08T07:26:00.400Z	38.03283	-121.9196667	19.44	2.01	0.32	0.68	0.182
2018-03-27T16:27:07.140Z	38.21	-121.8161667	22.86	2.61	0.3	0.4	0.143
2017-12-24T19:23:46.810Z	38.038	-121.8976667	17.92	2.26	0.19	0.24	0.194
2017-12-14T05:34:58.470Z	38.26167	-121.881	15.74	1.81	0.39	0.73	0.218
2017-12-14T05:14:45.580Z	38.26233	-121.8875	14.45	2.36	0.17	0.34	0.206
2017-10-19T10:40:51.100Z	38.01667	-122.0361667	17.04	1.66	0.36	0.39	0.202
2017-10-19T10:30:21.120Z	38.01533	-122.0391667	16.33	1.7	0.26	0.38	0.172
2017-10-19T05:01:35.800Z	38.01633	-122.0241667	16.11	1.53	0.32	0.47	0.243
2017-04-24T23:28:52.110Z	38.13183	-121.9203333	22.19	2.04	0.34	0.25	0.178
2017-04-24T22:59:09.360Z	38.1355	-121.9313333	22.87	1.87	0.45	0.3	0.182
2017-04-24T22:58:28.340Z	38.12467	-121.9451667	21.79	2.14	0.33	0.23	0.17
2016-11-06T03:00:14.410Z	38.121	-121.9531667	12.99	1.36	0.71	2.72	0.119
2016-05-12T20:32:14.460Z	38.19283	-121.8341667	10.52	2.33	0.74	1.28	0.49
2016-03-27T20:46:37.430Z	38.19283	-121.7745	23.93	2.06	0.53	0.34	0.332
2016-03-21T06:33:01.360Z	38.19983	-121.8003333	23.54	2.58	0.25	0.32	0.241
2016-02-27T03:21:09.850Z	38.09383	-121.9706667	18.9	1.97	0.46	0.55	0.174
2016-01-12T11:03:56.730Z	38.09683	-121.9218333	24.2	1.8	0.41	0.3	0.234
2016-01-12T05:46:52.140Z	38.104	-121.9166667	21.42	1.77	0.46	0.26	0.238
2016-01-12T04:34:55.130Z	38.096	-121.9038333	23.06	1.92	0.24	0.16	0.185
2016-01-12T04:24:20.040Z	38.10017	-121.925	24.13	2.89	0.35	0.73	0.203
2016-01-11T10:33:38.930Z	38.10583	-121.9316667	20.53	2.58	0.3	0.2	0.205
2016-01-04T21:35:31.160Z	38.07983	-121.919	20.34	2.06	0.66	0.25	0.189
2016-01-02T06:38:33.270Z	38.08567	-121.916	20.43	2.5	0.26	0.19	0.155
2016-01-02T04:29:29.230Z	38.10917	-121.9375	19.84	2.19	0.23	0.14	0.189
2015-11-05T06:40:45.910Z	38.22783	-121.7865	27.79	2.5	0.36	0.97	0.181
2015-06-02T03:52:54.550Z	38.119	-121.9403333	21.089	1.49	0.38	0.7	0.147
2015-02-16T00:25:45.150Z	38.01617	-121.8905	17.501	1.58	0.65	0.71	0.134
2015-01-23T23:00:43.640Z	37.99733	-121.8686667	13.709	2.14	0.25	0.42	0.196
2015-01-11T08:06:59.010Z	38.048	-121.9091667	19.868	2.54	0.2	0.34	0.139
2015-01-07T13:58:34.320Z	38.004	-121.9035	17.475	1.84	0.25	0.32	0.169
2014-10-05T17:57:00.550Z	38.0385	-121.9138333	19.175	1.8	0.22	0.27	0.233
2014-09-04T15:18:08.590Z	38.09133	-121.902	19.237	2.1	0.29	0.34	0.166
2014-08-15T15:52:19.860Z	37.9935	-121.8363333	17.52	1.78	0.54	0.43	0.228
2014-08-12T21:02:44.770Z	38.046	-121.883	16.811	2.19	0.19	0.27	0.171
2014-05-28T05:24:14.580Z	38.02783	-121.8868333	17.296	1.61	0.27	0.29	0.127
2014-03-10T10:48:50.020Z	38.11983	-121.9001667	18.679	2.2	0.4	0.33	0.137
2014-01-26T22:23:34.480Z	38.24083	-121.839	19.586	2.15	0.28	0.26	0.172
2013-09-07T13:10:20.020Z	38.07833	-121.923	3.203	1.44	0.49	0.9	0.102
2013-07-23T12:55:13.340Z	38.05483	-121.9186667	17.23	2.21	0.52	0.69	0.199
2013-06-27T09:09:08.290Z	38.1565	-121.939	20.328	2.46	0.53	0.41	0.162
2013-06-26T10:17:15.900Z	38.14733	-121.9126667	13.19	1.65	0.69	2.03	0.246
2013-06-26T08:03:31.700Z	38.15	-121.9265	19.558	2	0.45	0.29	0.163
2013-06-26T04:43:20.290Z	38.15167	-121.9316667	21.485	2.61	0.28	0.19	0.162
2013-06-25T11:15:13.890Z	38.1555	-121.9185	19.704	1.55	0.29	0.43	0.255
2013-06-24T22:44:39.820Z	38.15083	-121.928	15.75	1.41	0.43	1.97	0.182
2013-06-24T20:40:58.140Z	38.1555	-121.9196667	18.827	1.6	0.28	31.61	0.229
2013-06-24T20:05:59.200Z	38.15383	-121.9225	-0.12	1.71	0.61	0.55	0.199
2013-06-24T19:59:14.620Z	38.15033	-121.9196667	18.844	1.79	0.19	31.61	0.229
2013-03-11T12:16:42.220Z	38.02667	-121.8923333	14.631	1.47	0.66	1.13	0.234
2013-01-19T02:35:34.330Z	38.06417	-121.9343333	16.79	1.58	0.4	0.43	0.265
2013-01-18T17:55:28.100Z	38.02167	-121.762	19.79	1.78	1.47	0.29	0.191
2013-01-01T08:19:22.810Z	38.11183	-121.922	19.128	1.84	0.58	0.85	0.169

APPENDIX A.I-A. TABULATED SEISMISCITY HISTORY FOR STUDY AREA FROM 1969 TO END OF 2022

Date/time	Latitude	Longitude	Depth (km)	Magnitude	Horizontal Error (km)	Depth Error (km)	Magnitude Error
2012-11-18T11:40:04.400Z	38.13367	-121.8935	19.943	2.43	0.25	0.28	0.14
2012-11-15T04:45:33.460Z	38.0025	-121.8815	17.084	2.02	0.31	0.44	0.168
2012-11-05T07:54:13.160Z	38.038	-121.901	18.2	1.71	0.68	0.35	0.281
2012-08-20T05:20:34.930Z	37.99417	-121.8668333	18.225	2.09	0.32	0.22	0.161
2012-08-11T14:44:28.030Z	38.107	-121.8846667	19.174	1.44	0.69	0.6	0.164
2012-05-28T02:58:32.200Z	38.05817	-121.8918333	17.122	2.01	0.57	0.68	0.162
2012-05-12T21:44:30.200Z	38.12367	-121.892	21.796	1.81	0.52	0.47	0.176
2012-05-12T04:23:19.330Z	38.133	-121.8831667	20.629	2.32	0.3	0.17	0.152
2012-05-12T04:13:45.450Z	38.12467	-121.8918333	21.282	1.9	0.45	0.38	0.24
2012-05-11T18:36:49.180Z	38.11667	-121.9006667	20.277	1.93	0.59	0.44	0.156
2012-05-11T09:05:23.740Z	38.08167	-121.9333333	20.973	1.83	1.06	0.33	0.267
2012-05-08T03:28:15.500Z	38.08383	-121.9411667	19.469	2.12	0.64	0.22	0.148
2011-11-11T21:45:59.180Z	38.16167	-121.9083333	19.298	1.83	0.6	0.8	0.253
2011-11-02T17:32:05.460Z	38.1555	-121.9133333	20.271	2.76	0.49	0.38	0.141
2011-09-23T01:54:28.470Z	38.076	-121.9243333	14.471	1.54	0.57	0.8	0.156
2011-09-22T23:57:20.050Z	38.08817	-121.917	0.049	2.39	0.47	0.86	0.139
2011-04-08T04:28:13.550Z	38.07683	-121.865	16.009	1.92	0.42	0.89	0.172
2010-12-21T23:19:05.660Z	38.0235	-121.8615	15.44	1.65	1.16	0.52	0.182
2010-12-15T10:35:47.370Z	38.13583	-121.9178333	20.103	2.38	0.27	0.25	0.151
2010-12-15T10:23:30.940Z	38.14017	-121.9288333	18.423	2	0.29	0.21	0.157
2010-12-15T10:22:30.090Z	38.13483	-121.9203333	20.913	1.9	0.3	0.39	0.168
2010-11-19T06:41:32.420Z	38.00783	-121.9015	17.493	2.22	0.32	0.22	0.127
2010-10-13T06:29:31.430Z	38.09483	-121.985	21.008	1.52	0.36	0.73	0.112
2010-06-21T22:29:06.820Z	38.0785	-121.8705	20.462	2.13	0.25	0.23	0.186
2010-06-09T11:05:13.150Z	38.11167	-121.8776667	18.792	1.59	0.56	0.76	0.148
2010-06-08T16:55:52.940Z	38.092	-121.933	22.757	1.78	0.98	0.31	0.222
2010-03-01T20:03:11.840Z	38.05317	-121.8986667	19.147	2.51	0.2	0.21	0.167
2010-01-12T07:55:28.920Z	38.003	-121.8825	16.546	1.99	0.33	0.43	0.128
2009-12-18T22:38:07.670Z	38.0815	-121.8778333	16.323	1.51	0.38	0.88	0.126
2009-12-03T11:17:28.160Z	38.0275	-121.9873333	5.56	2.15	0.26	0.52	0.184
2009-11-23T02:27:40.040Z	38.07467	-121.9081667	22.084	1.62	0.55	0.34	0.141
2009-11-18T21:12:20.920Z	38.1025	-121.9065	22.922	1.79	1.13	0.28	0.216
2009-11-18T00:04:34.650Z	38.1415	-121.8603333	19.112	1.91	0.43	0.28	0.155
2009-09-30T14:31:13.510Z	38.04717	-121.8966667	18.767	1.89	0.3	0.46	0.169
2009-07-26T17:57:22.760Z	38.11783	-121.8763333	21.09	1.76	0.56	0.28	0.323
2009-07-26T17:52:12.680Z	38.1175	-121.8826667	22.663	2.16	0.36	0.16	0.229
2009-07-22T10:28:00.890Z	38.11633	-121.8876667	20.917	2.16	0.54	0.39	0.175
2009-07-20T13:25:43.930Z	38.01967	-121.9216667	16.489	1.7	0.91	0.49	0.253
2009-07-17T12:28:27.450Z	38.233	-121.8338333	21.465	2.52	0.47	0.25	0.175
2009-06-30T09:08:52.100Z	38.11017	-121.8448333	4.95	1.89	1.63	31.61	0.106
2009-06-30T09:08:43.040Z	38.10783	-121.887	19.03	2.25	0.33	0.25	0.052
2009-06-04T12:49:48.960Z	38.17533	-121.8673333	21.068	2.57	0.35	0.2	0.125
2009-06-02T01:02:53.820Z	38.20683	-121.834	21.275	2.8	0.3	0.19	0.176
2009-05-28T18:25:26.400Z	38.04583	-121.8648333	18.056	1.91	0.34	0.39	0.138
2009-05-18T12:12:59.670Z	38.09317	-121.9228333	21.358	1.62	1.43	0.61	0.176
2009-05-18T09:18:27.340Z	38.1265	-121.9061667	23.263	1.71	0.49	0.36	0.167
2009-05-03T16:39:37.060Z	38.085	-121.9955	18.413	1.71	0.33	0.54	0.15
2009-04-23T14:13:28.790Z	38.006	-122.04	4.769	0.83	0.93	31.61	0.282
2009-04-21T08:42:41.810Z	38.026	-121.8431667	11.126	1.56	0.46	0.8	0.166
2009-04-17T06:27:06.420Z	38.08383	-121.992	18.718	1.68	0.29	0.68	0.206
2009-04-16T23:48:49.820Z	38.08833	-122.0033333	19.038	1.73	0.74	1.75	0.078
2009-04-16T23:40:36.990Z	38.08383	-121.9813333	17.913	2.8	0.21	0.27	0.101
2009-04-16T23:22:15.260Z	38.088	-122.0006667	20.023	1.52	0.61	1.19	0.195
2009-04-09T01:01:20.120Z	38.05233	-121.8845	18.823	1.75	0.4	0.57	0.124
2009-04-09T00:00:20.340Z	38.053	-121.882	17.198	1.88	0.42	0.32	0.146

APPENDIX A.I-A. TABULATED SEISMISCITY HISTORY FOR STUDY AREA FROM 1969 TO END OF 2022

Date/time	Latitude	Longitude	Depth (km)	Magnitude	Horizontal Error (km)	Depth Error (km)	Magnitude Error
2009-04-07T18:45:19.910Z	38.05333	-121.8906667	19.023	2.13	0.39	0.32	0.165
2009-02-01T01:45:10.640Z	38.0465	-121.8828333	22.187	1.55	0.78	0.42	0.2
2009-01-20T15:50:22.640Z	38.047	-121.901	19.212	2.09	0.57	0.31	0.115
2008-12-29T16:22:51.420Z	38.24317	-121.878	20.31	1.43	0.54	0.88	0.037
2008-11-20T10:06:49.250Z	38.00233	-121.8588333	18.051	1.45	0.54	0.36	0.189
2008-11-11T04:46:34.490Z	38.1575	-121.9465	21.473	2.11	0.33	0.21	0.174
2008-11-11T01:26:45.210Z	38.19117	-121.9683333	4.091	1.27	1.14	4.15	0.174
2008-11-10T09:43:35.850Z	38.162	-121.9478333	21.333	1.8	0.49	0.59	0.163
2008-11-10T04:28:38.850Z	38.1685	-121.9611667	20.687	2.19	0.33	0.26	0.181
2008-11-10T03:09:07.520Z	38.15983	-121.9595	22.638	1.92	0.55	0.36	0.211
2008-11-10T02:06:21.280Z	38.17167	-121.9561667	20.646	1.71	0.36	0.65	0.207
2008-11-10T02:03:11.680Z	38.16983	-121.9588333	22.133	1.91	0.42	0.16	0.197
2008-11-10T01:38:19.860Z	38.16833	-121.9431667	20.853	2.42	0.33	0.28	0.159
2008-11-10T01:35:44.700Z	38.16117	-121.9566667	22.953	2.39	0.38	0.24	0.135
2008-11-08T01:21:53.950Z	38.04867	-121.9068333	20.882	1.8	0.54	0.67	0.167
2008-11-07T18:54:29.070Z	38.1965	-121.9096667	4.665	1.14	2.59	6.8	0.123
2008-11-07T00:47:44.570Z	38.19183	-121.9666667	0.626	1.31	0.39	2.28	0.165
2008-11-06T22:57:34.870Z	38.161	-121.9535	21.893	2.95	0.27	0.19	0.235
2008-11-06T22:57:08.370Z	38.1655	-121.951	21.296	2.17	0.28	0.35	0.116
2008-10-31T03:21:31.420Z	38.16967	-121.9616667	21.855	1.42	0.53	0.88	0.13
2008-10-31T02:55:56.870Z	38.16983	-121.9605	24.345	1.61	0.42	0.61	0.143
2008-10-06T09:51:13.960Z	38.08083	-121.9618333	19.918	1.5	0.92	1.95	0.081
2008-07-16T17:00:50.340Z	38.05083	-122.008	20.709	1.56	0.42	1.13	0.166
2008-07-16T16:36:51.790Z	38.05567	-122.0136667	19.358	1.8	0.31	0.18	0.213
2008-07-16T05:36:08.810Z	38.06717	-122.0183333	13.553	0.87	0.72	3.07	0.157
2008-07-16T05:24:55.700Z	38.05517	-122.0046667	19.584	1.62	0.32	0.33	0.405
2008-07-16T05:23:51.480Z	38.05133	-121.9995	19.2	2.09	0.42	0.27	0.191
2008-07-16T05:14:58.740Z	38.056	-122.0063333	19.308	2.14	0.27	0.22	0.125
2008-07-16T05:06:14.540Z	38.05383	-122.0123333	19.01	1.55	0.37	0.3	0.192
2008-07-16T04:28:12.990Z	38.0535	-122.0085	19.224	1.83	0.26	0.19	0.178
2008-07-16T04:22:07.870Z	38.05167	-122.0141667	18.563	1.66	0.39	0.4	0.196
2008-07-12T18:38:53.260Z	38.02967	-122.0306667	16.641	1.14	0.85	0.38	0.07
2008-07-12T09:24:27.270Z	38.051	-122.007	19.034	2.34	0.26	0.18	0.114
2008-07-11T03:08:09.680Z	38.05483	-121.9848333	18.259	2.14	0.64	0.46	0.168
2008-07-11T00:13:31.890Z	38.05633	-122.0215	18.625	1.74	0.7	0.3	0.261
2008-07-07T18:42:45.640Z	37.99633	-121.8755	15.506	1.64	0.39	0.41	0.061
2008-04-28T23:55:32.000Z	38.06167	-121.8793333	18.829	1.77	4.63	3.08	0.144
2008-01-02T22:50:32.190Z	38.04683	-121.8775	17.832	2.53	0.27	0.32	0.158
2007-11-23T22:17:09.050Z	38.111	-121.9301667	20.732	2.05	0.31	0.25	0.127
2007-11-16T22:35:41.640Z	38.05133	-121.8816667	17.067	1.78	0.43	0.4	0.075
2007-11-16T20:15:42.410Z	38.04967	-121.8595	16.786	2.15	0.42	0.38	0.098
2007-10-28T08:02:22.730Z	38.0685	-121.8706667	17.872	1.92	0.39	0.53	0.143
2007-10-24T06:48:49.520Z	37.99317	-121.8685	15.177	1.6	0.25	0.36	0.152
2007-09-28T07:14:28.720Z	38.12133	-121.8685	15.698	1.75	2.04	0.39	0.073
2007-07-18T14:30:44.460Z	38.0555	-121.878	17.975	1.46	0.52	0.94	0.078
2007-04-08T10:00:30.810Z	38.2155	-121.908	0.073	1.83	0.77	4.14	0.19
2007-03-05T21:31:45.700Z	38.04167	-121.8928333	16.087	1.56	1.26	1.35	0.001
2007-03-05T21:26:56.290Z	38.07067	-121.8743333	15.822	2.52	0.34	0.65	0.112
2007-03-05T18:49:00.910Z	38.08167	-121.8418333	19.207	1.7	0.66	0.67	0.216
2007-03-05T15:32:53.150Z	38.06233	-121.8835	16.972	1.88	0.27	0.34	0.22
2007-03-05T15:27:46.310Z	38.05933	-121.8813333	17.152	2.81	0.27	0.33	0.145
2007-02-17T09:32:29.430Z	38.07617	-121.9505	17.722	2.1	0.45	0.81	0.576
2007-02-08T01:06:14.500Z	38.125	-121.8763333	22.447	1.78	0.48	0.42	0.077
2007-01-02T00:43:10.540Z	38.06	-121.8796667	18.672	1.8	0.39	0.5	0.29
2007-01-01T21:43:42.970Z	38.0615	-121.8735	17.677	2.01	0.33	0.36	0.12

APPENDIX A.I-A. TABULATED SEISMISCITY HISTORY FOR STUDY AREA FROM 1969 TO END OF 2022

Date/time	Latitude	Longitude	Depth (km)	Magnitude	Horizontal Error (km)	Depth Error (km)	Magnitude Error
2007-01-01T21:42:14.050Z	38.10633	-121.8393333	22.072	1.74	0.54	0.61	0.127
2006-08-06T06:00:52.050Z	38.1105	-121.8783333	20.202	2.19	0.38	0.25	0.11
2006-07-29T15:34:51.530Z	38.02833	-121.865	16.126	2.01	0.49	0.58	0.17
2005-07-07T20:30:32.680Z	38.23133	-121.9238333	4.77	1.44	6.79	47.97	
2005-06-13T13:56:32.810Z	38.17467	-121.9763333	4.243	1.75	0.48	9.92	0.13
2005-06-11T12:51:51.150Z	38.17683	-122.023	4.585	1.43	3.57	11.68	0.05
2005-06-08T10:41:27.790Z	38.01233	-122.018	12.24	2.89	2.64	3.16	1.03
2005-01-27T07:00:16.470Z	38.20383	-121.8943333	15.293	2.2	0.42	0.6	0.1
2005-01-27T02:19:33.820Z	38.21133	-122.0183333	14.159	2.16	1.04	1.5	0.09
2005-01-26T21:20:03.180Z	38.20783	-121.8953333	17.493	2.78	0.27	0.36	0.11
2004-09-09T05:32:51.880Z	38.185	-121.7855	22.445	2.23	0.46	0.22	0.15
2004-09-07T11:46:33.550Z	38.196	-121.9005	4.77	1.84	0.58	7.12	0.08
2004-09-07T10:16:01.670Z	38.19983	-121.8943333	2.9	2.12	0.81	12.02	0.05
2004-07-21T10:41:24.830Z	38.00067	-121.9515	5.061	1.83	18.07	40.84	
2004-06-17T21:57:30.380Z	38.04717	-121.8738333	18.612	1.97	0.71	0.53	0.11
2004-04-16T23:00:16.580Z	38.05183	-121.8546667	18.43	2.35	0.27	0.22	0.07
2004-04-13T05:29:28.740Z	38.14783	-121.8088333	14.204	1.84	0.35	0.28	0.1
2004-01-30T15:24:49.120Z	38.05467	-121.8591667	17.28	2.25	0.4	0.52	0.09
2003-10-22T07:39:20.640Z	38.0455	-122.0355	17.711	1.61	0.51	0.86	0.18
2003-10-13T03:11:12.950Z	38.169	-122.0268333	1.969	2.15	0.76	6.54	0.74
2003-10-11T12:53:03.900Z	38.21183	-122.0001667	54.206	2	31.05	29.51	0.05
2003-08-07T16:03:18.420Z	38.06783	-121.929	21.569	2.07	1.39	0.33	
2003-04-14T08:48:46.940Z	38.03367	-122.0318333	19.726	1.4	0.77	1.11	0.12
2003-04-12T11:05:25.620Z	38.0385	-122.0391667	20.421	1.58	0.52	0.65	0.1
2003-04-12T07:03:46.910Z	38.0335	-122.0231667	20.656	1.56	0.49	0.91	0.09
2003-04-12T02:19:25.200Z	38.044	-122.0368333	17.501	1.63	0.55	1.37	0.44
2003-04-11T22:34:23.850Z	38.0455	-122.0256667	19.271	1.45	0.95	1.1	
2003-04-11T07:35:06.640Z	38.01317	-121.9093333	15.547	1.35	0.43	0.46	0.04
2003-04-11T04:06:41.130Z	38.00117	-121.9135	12.167	1.22	1.34	1.38	
2003-03-30T13:47:04.340Z	37.99617	-121.8715	14.291	1.95	0.29	0.51	0.12
2003-02-17T03:54:47.800Z	38.14417	-122.0175	4.878	1.67	1.48	5.93	0.17
2002-10-03T02:13:49.730Z	38.122	-121.8516667	22.225	1.68	0.81	0.34	0.28
2002-10-02T16:54:31.830Z	38.123	-121.8563333	21.634	2.47	0.31	0.18	0.12
2002-08-16T06:06:43.990Z	38.08767	-121.8771667	20.235	2.63	0.2	0.19	0.09
2002-07-21T23:07:12.750Z	38.061	-121.8246667	6.855	1.29	0.57	7.62	0.27
2002-06-14T14:56:31.690Z	38.18967	-121.9391667	4.873	1.76	51.24	57.62	
2002-05-08T14:59:36.110Z	38.22383	-121.8375	17.43	3.6	0.22	0.31	
2002-03-19T17:13:32.440Z	38.24183	-121.837	17.059	2.05	0.85	0.92	0.15
2002-03-19T16:08:39.960Z	38.24533	-121.832	17.61	2.31	0.3	0.35	0.21
2002-01-24T16:36:49.400Z	38.05817	-121.8733333	16.926	2.46	0.36	0.38	0.1
2001-08-29T16:11:58.020Z	38.13617	-121.845	15.265	1.89	0.57	0.94	0.16
2001-08-25T13:27:29.860Z	38.04867	-121.8365	19.222	1.46	0.62	0.3	0.02
2001-08-25T13:21:14.460Z	38.05933	-121.8358333	20.963	2.66	0.32	0.18	0.09
2001-05-29T02:35:11.390Z	38.003	-121.882	19.022	1.88	0.29	0.45	0.16
2001-05-28T16:09:04.070Z	38.06983	-121.8955	19.517	1.97	0.28	0.49	0.11
2001-05-19T23:58:22.160Z	38.08583	-121.8965	22.192	1.65	0.54	0.61	0.21
2001-04-14T20:11:28.730Z	37.99833	-121.856	18.194	1.85	0.26	0.35	0.21
2001-04-14T16:07:44.050Z	37.99683	-121.8541667	18.034	2.47	0.17	0.2	0.11
2001-01-31T08:38:07.170Z	38.0015	-121.861	16.654	2.45	0.19	0.28	0.12
2001-01-14T12:30:42.100Z	38.05633	-121.8523333	14.555	1.65	0.51	0.72	0.09
2000-11-11T18:53:39.160Z	38.24417	-121.8306667	18.804	1.81	0.38	0.45	0.08
2000-07-24T11:31:23.390Z	38.042	-121.8551667	18.131	1.76	0.68	0.27	0.25
2000-07-17T11:42:52.550Z	38.03483	-121.9585	4.983	1.37	3.51	7.49	0.09
2000-07-05T14:35:15.900Z	38.0505	-121.8393333	14.957	2.44	0.18	0.28	0.1
2000-04-14T04:24:27.810Z	38.02533	-121.8985	16.095	1.53	0.33	0.32	0.11

APPENDIX A.I-A. TABULATED SEISMISCITY HISTORY FOR STUDY AREA FROM 1969 TO END OF 2022

Date/time	Latitude	Longitude	Depth (km)	Magnitude	Horizontal Error (km)	Depth Error (km)	Magnitude Error
2000-01-07T23:20:55.110Z	38.218	-121.8275	17.589	2.24	0.18	0.27	0.11
1999-12-27T17:43:44.680Z	38.22067	-121.8223333	18.629	2.21	0.36	0.44	0.27
1999-09-29T09:08:22.340Z	38.1195	-121.8741667	15.721	2.05	0.58	0.39	0.25
1999-09-03T00:46:54.360Z	38.09667	-121.8693333	18.591	1.84	0.33	0.36	0.26
1999-06-19T18:57:51.830Z	38.0405	-121.8445	16.722	1.88	0.39	0.3	0.189
1999-05-21T02:37:37.240Z	38.0605	-121.8668333	15.905	1.97	0.33	0.57	0.22
1999-04-04T18:12:15.380Z	38.092	-121.8838333	20.145	3.19	0.19	0.17	0.1
1999-04-02T07:47:27.990Z	38.094	-121.8616667	21.095	2.27	0.27	0.2	0.16
1998-12-13T03:06:03.000Z	38.07517	-121.8611667	18.303	1.67	0.95	0.71	0.2
1998-09-12T12:46:28.400Z	37.99967	-121.855	19.162	2.45	0.2	0.21	0.15
1998-05-22T11:53:26.040Z	38.00367	-121.9118333	16.67	1.47	0.37	0.27	0.22
1998-04-09T00:53:17.290Z	38.06483	-121.8528333	16.541	2.1	0.31	0.44	0.16
1997-11-30T20:40:37.450Z	38.102	-121.8815	17.601	1.8	0.45	0.43	0.21
1997-11-30T04:49:37.570Z	38.08917	-121.8663333	20.183	2.49	0.19	0.14	0.12
1997-11-28T10:29:00.110Z	38.084	-121.8541667	20.49	1.99	0.35	0.24	0.11
1997-09-18T21:19:04.860Z	38.01033	-121.8583333	17.472	2.31	0.16	0.25	0.17
1997-07-30T20:28:22.200Z	38.00733	-121.9156667	15.092	1.89	0.35	0.25	0.3
1997-07-06T05:10:48.600Z	38.13717	-121.8415	13.066	1.55	1.04	0.95	0.26
1997-07-05T05:09:42.850Z	38.27083	-121.8303333	6.739	1.76	2.72	7.62	0.31
1997-06-01T13:43:04.110Z	38.16467	-121.8913333	19.125	2.44	0.18	0.22	0.12
1997-05-23T04:41:36.930Z	38.14867	-121.7961667	16.735	2.17	0.24	0.28	0.16
1997-04-26T00:30:06.320Z	38.166	-121.9665	5.718	1.76	0.33	10.66	0.04
1997-04-22T23:30:51.880Z	38.0715	-121.8488333	16.935	1.83	0.36	0.44	0.17
1997-04-05T19:03:20.930Z	38.16817	-121.941	21.035	2.17	0.24	0.58	0.17
1997-04-04T10:56:56.930Z	38.17317	-121.9558333	21.313	2	0.53	0.74	0.2
1997-04-04T10:33:29.310Z	38.189	-121.9555	6.435	1.64	0.34	8.36	0.21
1997-04-04T00:25:25.650Z	38.189	-121.9548333	7.755	1.71	0.62	7.86	0.25
1997-04-02T22:27:08.940Z	38.15717	-121.9396667	21.365	2.7	0.32	0.19	0.14
1997-04-02T12:14:12.370Z	38.14733	-121.9211667	21.725	2.51	0.2	0.26	0.13
1997-04-01T19:50:41.680Z	38.19017	-121.9778333	4.913	2.21	1.09	21.77	0.15
1997-04-01T18:37:18.590Z	38.15633	-121.9381667	21.375	3.38	0.19	0.14	0.13
1997-04-01T11:25:54.450Z	38.15917	-121.9363333	21.765	2.73	0.17	0.15	0.1
1997-04-01T05:27:58.520Z	38.1915	-121.9588333	2.317	1.97	0.54	6.08	0.22
1997-04-01T03:00:58.590Z	38.191	-121.9586667	4.765	1.71	0.65	7.42	0.35
1997-04-01T01:51:08.030Z	38.15867	-121.9605	18.048	2.05	0.72	1.09	0.09
1997-04-01T01:36:54.860Z	38.15083	-121.93	21.385	3.65	0.22	0.16	0.14
1997-03-30T07:40:40.180Z	38.16183	-121.9353333	22.575	2.13	0.27	0.43	0.14
1997-03-30T02:38:26.350Z	38.16017	-121.9338333	21.493	2.01	0.32	0.63	0.11
1997-03-29T13:05:22.580Z	38.16533	-121.9435	18.143	2.2	0.24	0.86	0.16
1997-03-29T08:20:46.670Z	38.15183	-121.9276667	21.595	2.41	0.31	0.24	0.12
1997-03-28T13:03:47.560Z	38.16217	-121.9286667	23.615	2.21	0.39	0.57	0.12
1997-03-28T03:35:58.810Z	38.18167	-121.9748333	4.722	2.08	1.31	20.29	0.06
1997-03-27T22:53:07.620Z	38.15183	-121.934	21.465	3.46	0.2	0.17	0.13
1997-03-27T22:47:53.010Z	38.151	-121.9328333	21.675	3.6	0.19	0.17	0.11
1997-03-27T22:16:18.770Z	38.15867	-121.9346667	21.495	2.65	0.13	0.14	0.09
1997-03-27T20:40:00.260Z	38.15367	-121.9228333	21.165	2.3	0.33	0.4	0.16
1997-03-27T18:01:43.170Z	38.1555	-121.9351667	21.645	3.38	0.2	0.16	0.11
1997-03-27T17:16:42.790Z	38.15783	-121.9271667	21.605	3.41	0.23	0.14	0.09
1997-03-27T17:07:37.800Z	38.15283	-121.9301667	21.495	2.51	0.13	0.17	0.14
1997-03-27T16:35:19.120Z	38.159	-121.9195	20.942	1.84	0.9	0.75	0.24
1997-03-27T15:39:49.000Z	38.151	-121.9306667	21.425	3.7	0.22	0.19	
1997-03-27T14:01:24.230Z	38.14983	-121.9315	21.455	3.48	0.21	0.16	0.1
1997-03-27T13:38:08.840Z	38.14983	-121.9273333	21.145	3.33	0.17	0.14	0.09
1997-03-27T13:15:33.680Z	38.14817	-121.918	21.883	2.18	0.79	0.72	0.23
1997-03-27T11:30:06.990Z	38.15	-121.9335	21.335	3.57	0.21	0.17	0.11

APPENDIX A.I-A. TABULATED SEISMISCITY HISTORY FOR STUDY AREA FROM 1969 TO END OF 2022

Date/time	Latitude	Longitude	Depth (km)	Magnitude	Horizontal Error (km)	Depth Error (km)	Magnitude Error
1997-03-27T11:11:24.510Z	38.1505	-121.9268333	21.835	2.91	0.2	0.18	0.12
1997-03-27T10:57:19.650Z	38.1625	-121.9735	6.092	2.04	1.01	14.22	0.06
1997-03-27T10:26:35.300Z	38.14917	-121.9286667	21.695	2.92	0.17	0.16	0.12
1997-03-27T10:17:05.600Z	38.15417	-121.9295	21.885	2.13	0.16	0.24	0.14
1997-03-27T10:10:45.140Z	38.15067	-121.9286667	21.365	3.35	0.15	0.1	0.12
1997-03-27T09:11:18.570Z	38.153	-121.9291667	22.625	2.16	0.37	0.29	0.15
1997-03-26T15:34:59.510Z	38.15167	-121.93	21.485	2.81	0.13	0.17	0.14
1997-03-26T14:50:46.580Z	38.16917	-121.9543333	19.215	2.04	0.6	0.67	0.21
1997-03-26T14:06:24.530Z	38.15683	-121.9306667	22.555	2.58	0.18	0.18	0.16
1997-03-26T14:01:41.710Z	38.15533	-121.9308333	21.335	2.27	0.14	0.29	0.13
1997-03-26T12:34:29.940Z	38.156	-121.949	20.407	2.18	0.43	0.81	0.1
1997-03-26T12:06:39.770Z	38.04217	-121.9926667	10.717	1.83	2.82	3.66	0.25
1997-03-26T12:05:56.600Z	38.1735	-121.9331667	23.545	2.08	0.69	0.39	0.14
1996-10-16T00:37:10.060Z	38.07133	-121.8668333	14.205	2.46	0.23	0.4	0.1
1996-08-21T10:06:40.870Z	37.99733	-121.8621667	16.862	1.36	0.46	1.18	0.03
1996-07-20T12:26:41.900Z	38.13683	-121.8518333	24.915	1.92	1.24	1.09	0.18
1996-07-17T11:06:30.650Z	38.112	-121.8583333	21.385	2.79	0.24	0.13	0.13
1996-07-17T05:57:41.470Z	38.11667	-121.8635	19.043	1.84	0.88	0.43	0.18
1996-07-16T15:06:37.010Z	38.12017	-121.8558333	21.385	2.42	0.27	0.18	0.15
1996-07-15T21:44:36.350Z	38.1155	-121.86	20.965	3.22	0.26	0.18	0.12
1996-07-15T19:39:47.350Z	38.1145	-121.8576667	21.465	2.62	0.32	0.2	0.1
1996-07-08T17:25:57.370Z	38.12267	-121.8596667	21.365	2.17	0.28	0.18	0.18
1996-04-09T10:01:48.720Z	38.01283	-121.88	16.201	1.87	0.29	0.31	0.13
1996-03-07T12:15:21.260Z	38.00967	-121.8451667	18.072	2.7	0.17	0.22	0.14
1996-03-07T11:41:35.790Z	38.008	-121.8678333	17.941	1.74	0.59	0.43	0.3
1996-03-07T11:36:59.240Z	38.00767	-121.8606667	18.352	2.17	0.32	0.46	0.19
1996-03-07T11:31:49.360Z	38.00583	-121.8676667	18.112	1.79	0.36	0.23	0.16
1996-03-07T09:21:47.280Z	38.0135	-121.8638333	17.286	1.71	0.6	0.79	0.23
1996-03-07T09:00:29.190Z	38.01083	-121.8576667	17.562	2.14	0.16	0.3	0.2
1995-12-05T10:02:53.650Z	38.06633	-121.8393333	17.865	2.02	0.46	0.64	0.19
1995-10-27T07:21:44.550Z	38.0495	-121.8545	13.175	1.79	0.86	1.56	0.12
1995-07-31T17:48:34.990Z	38.066	-121.9011667	21.94	1.74	0.72	0.86	0.17
1995-07-08T21:33:03.340Z	38.01683	-121.895	17.186	1.57	0.54	0.43	0.18
1995-06-26T13:15:31.620Z	38.224	-121.7928333	14.76	2.06	0.4	0.32	0.21
1995-06-06T05:28:22.390Z	38.05	-121.8423333	19.081	2.14	0.24	0.28	0.16
1995-05-25T14:15:28.790Z	38.23683	-121.7821667	15.169	2.41	0.31	0.33	0.15
1995-01-12T07:08:19.770Z	38.00217	-121.8566667	18.192	2.03	0.3	0.51	0.19
1994-12-19T03:25:10.420Z	38.06233	-121.9025	16.625	1.73	0.73	0.86	0.12
1994-11-20T20:00:28.250Z	38.06567	-121.8625	4.655	1.49	1.67	7.38	0.11
1994-11-18T21:39:27.910Z	38.084	-122.0018333	-0.135	1.91	1.61	6.13	0.19
1994-10-31T01:53:10.290Z	38.0065	-122.036	18.717	1.47	1.06	1.22	0.06
1994-07-11T18:25:48.810Z	38.08783	-121.8703333	18.565	2.71	0.27	0.19	0.15
1994-06-01T22:46:29.580Z	38.02033	-121.9793333	0.938	1.92	2.35	9	0.13
1994-05-25T06:57:49.180Z	38.07817	-121.8643333	19.545	2.08	0.31	0.35	0.23
1994-05-10T18:26:35.800Z	38.1045	-121.8766667	20.765	2.68	0.3	0.26	0.14
1994-01-28T13:10:53.580Z	38.0715	-121.9326667	4.817	1.76	1.95	33.89	0.55
1993-11-16T01:12:16.930Z	38.02233	-121.8743333	20.492	1.95	0.25	0.55	0.26
1993-09-06T21:14:32.710Z	38.0005	-121.86	17.364	2.12	0.34	0.23	0.13
1993-08-09T14:32:24.310Z	38.1055	-121.8703333	19.213	2.25	0.2	0.17	0.11
1993-07-28T05:58:14.190Z	38.03783	-121.9231667	7.655	1.15	0.58	5.61	0.51
1993-07-15T03:37:03.240Z	38.03017	-121.8906667	3.164	1.8	0.55	5.15	0.2
1993-06-03T19:17:47.060Z	38.12867	-121.855	19.594	1.91	0.68	0.35	0.22
1993-04-19T03:24:33.270Z	38.22533	-122.0016667	4.769	1.55	0.73	11.53	0.29
1993-02-15T08:14:18.750Z	38.11117	-121.8725	20.185	1.83	0.28	0.34	0.18
1993-02-05T00:17:33.350Z	38.12383	-121.8583333	22.615	2.15	1.42	3.17	0.21

APPENDIX A.I-A. TABULATED SEISMISCITY HISTORY FOR STUDY AREA FROM 1969 TO END OF 2022

Date/time	Latitude	Longitude	Depth (km)	Magnitude	Horizontal Error (km)	Depth Error (km)	Magnitude Error
1992-11-23T23:05:56.540Z	38.07667	-121.8533333	16.645	2.37	0.23	0.21	0.13
1992-11-23T20:59:55.560Z	38.07617	-121.858	17.735	3.26	0.19	0.22	0.09
1992-10-20T10:54:42.920Z	38.1335	-121.843	26.264	1.76	1.88	1.63	0.26
1992-10-04T05:02:46.770Z	38.01867	-121.8873333	15.521	1.95	0.31	0.57	0.19
1992-10-04T03:46:39.840Z	38.01583	-121.8918333	15.291	2.25	0.23	0.29	0.14
1992-09-01T01:17:29.310Z	38.139	-121.8916667	23.515	2.15	0.47	0.45	0.22
1992-08-20T03:52:27.010Z	38.1355	-121.9098333	20.285	2.23	0.19	0.28	0.1
1992-08-20T03:35:47.100Z	38.13967	-121.9093333	20.885	2.2	0.34	0.5	0.17
1992-08-20T02:31:06.640Z	38.13283	-121.9125	20.005	3.34	0.23	0.2	0.21
1992-08-20T02:30:59.180Z	38.13083	-121.8973333	22.245	1.57	0.3	0.37	0.68
1992-08-20T02:19:14.310Z	38.13517	-121.909	20.715	2.3	0.45	0.25	0.17
1992-08-20T01:25:22.530Z	38.13933	-121.913	21.015	2.11	0.31	0.23	0.22
1992-08-20T01:21:01.620Z	38.13583	-121.9036667	21.665	2.24	0.43	0.45	0.16
1992-08-01T22:45:02.420Z	38.106	-121.8828333	19.455	2.1	0.33	0.26	0.1
1992-03-15T22:17:59.410Z	38.06617	-121.8566667	20.205	2.36	0.53	0.36	0.12
1992-02-26T06:32:05.610Z	37.99517	-122.0416667	20.811	1.57	0.84	1.74	0.04
1992-02-25T20:06:42.740Z	38.10633	-121.862	-0.115	2.25	2.29	5.99	0.22
1992-02-01T23:38:37.280Z	38.1915	-121.72	9.991	2.03	0.88	1.09	0.03
1991-12-02T11:00:36.610Z	38.05733	-121.9068333	3.232	1.32	0.34	1.8	0.09
1991-09-07T10:38:59.060Z	38.045	-121.9053333	-0.284	0.91	1.6	31.61	0.24
1991-07-25T23:55:08.820Z	38.21567	-121.9228333	4.563	1.61	3.14	8.4	0.05
1991-07-25T17:57:18.910Z	38.07	-121.9148333	3.815	1.9	1.37	13.16	0.27
1991-07-03T05:17:01.740Z	38.09117	-121.9255	15.045	2.43	0.25	0.35	0.14
1991-07-03T05:13:35.970Z	38.088	-121.9276667	14.505	2.24	0.22	0.37	0.15
1991-07-02T18:05:11.840Z	38.08467	-121.9031667	4.545	1.81	2.94	7.23	0.1
1991-04-30T22:14:24.910Z	38.05567	-121.9635	13.004	1.86	1.24	1.12	0.59
1991-03-17T02:40:39.190Z	38.0525	-121.8665	16.181	1.94	0.38	0.5	0.12
1991-01-21T01:03:10.580Z	38.22883	-121.8301667	16.769	2.42	0.26	0.31	0.15
1991-01-19T19:01:48.290Z	38.0025	-121.8628333	17.192	1.82	0.45	0.67	0.25
1990-10-09T18:32:23.830Z	38.262	-121.8791667	4.663	1.87	0.9	8.26	0.14
1990-09-28T20:42:24.440Z	38.00767	-121.8658333	20.062	1.89	0.52	1.07	0.18
1990-09-05T19:16:01.210Z	38.00867	-121.9823333	7.492	1.61	0.79	1.51	0.09
1990-08-14T09:02:05.370Z	37.9955	-121.8613333	16.032	1.79	0.54	0.45	0.13
1990-05-20T23:41:15.500Z	38.0025	-121.8465	17.205	2.27	0.45	0.34	0.23
1990-04-28T05:08:45.680Z	38.1025	-121.974	8.776	2.24	6.19	2.14	0.06
1990-04-18T14:03:04.300Z	38.11367	-121.8631667	20.755	2.52	0.58	0.42	0.19
1990-04-14T00:05:56.150Z	38.11817	-121.8631667	20.855	2.08	0.78	0.46	0.11
1990-04-13T12:17:48.760Z	38.13983	-121.8443333	17.567	1.88	0.92	0.62	0.07
1990-03-22T02:54:22.420Z	38.0175	-121.8456667	0.342	2.06	0.93	5.62	0.27
1990-02-28T06:15:59.210Z	38.03617	-121.8678333	19.222	1.98	0.56	1.12	0.12
1989-10-15T11:52:17.240Z	38.17633	-121.9461667	4.897	1.49	1.13	7.44	0.31
1989-10-02T11:20:19.540Z	38.147	-121.9135	21.371	2.7	0.32	0.21	0.14
1989-10-02T08:13:56.240Z	38.13783	-121.923	1.957	1.55	0.68	12.34	0.15
1989-10-01T21:41:58.640Z	38.14533	-121.9371667	17.655	2.54	0.36	0.38	0.14
1989-10-01T21:13:34.020Z	38.1465	-121.9268333	20.695	2.04	0.39	0.5	0.23
1989-10-01T15:23:33.380Z	38.145	-121.8953333	2.653	1.85	1.36	20.71	0.16
1989-10-01T14:17:29.400Z	38.14583	-121.9203333	21.975	2.14	0.36	0.33	0.23
1989-10-01T13:38:28.500Z	38.13117	-121.9693333	0.925	1.78	1.17	22.05	0.22
1989-10-01T13:21:56.850Z	38.13733	-121.9371667	6.167	1.87	1.14	12.07	0.18
1989-10-01T13:19:27.500Z	38.164	-121.9251667	15.273	3.2	0.32	0.57	
1989-10-01T13:19:05.290Z	38.14067	-121.9083333	4.594	1.77	0.95	8.64	0.28
1989-10-01T13:10:24.280Z	38.141	-121.9315	17.323	3	0.24	0.28	
1989-10-01T13:04:05.930Z	38.14917	-121.9038333	18.203	2.39	0.31	0.34	0.12
1989-10-01T12:50:10.390Z	38.1425	-121.9015	13.773	2.13	0.92	0.59	0.14
1989-10-01T12:22:20.300Z	38.13467	-121.9411667	14.124	2.17	1.14	0.54	0.12

APPENDIX A.I-A. TABULATED SEISMISCITY HISTORY FOR STUDY AREA FROM 1969 TO END OF 2022

Date/time	Latitude	Longitude	Depth (km)	Magnitude	Horizontal Error (km)	Depth Error (km)	Magnitude Error
1989-10-01T12:21:37.360Z	38.155	-121.899	16.303	2.7	0.34	0.35	0.18
1989-10-01T11:37:49.160Z	38.13333	-121.9161667	2.913	1.97	1.1	11.69	0.04
1989-10-01T10:48:45.210Z	38.13733	-121.8906667	2.263	1.96	0.88	5.9	0.18
1989-09-11T16:20:35.740Z	38.084	-121.8656667	19.465	2.87	0.22	0.19	0.15
1989-07-03T13:54:47.520Z	38.06233	-121.8873333	16.619	2.19	0.53	0.35	0.17
1989-07-01T02:21:16.260Z	38.19233	-121.9563333	4.237	1.69	0.59	7.07	0.28
1989-06-30T19:06:15.400Z	38.18133	-121.949	16.678	1.67	1.25	2.14	0.14
1989-06-25T07:23:38.380Z	38.06117	-121.8583333	18.765	2	0.31	0.43	0.2
1989-06-24T11:59:38.620Z	38.05967	-121.8651667	17.856	2.66	0.21	0.24	0.12
1989-06-24T09:35:30.080Z	38.06217	-121.8745	17.179	2.28	0.45	0.3	0.15
1989-06-22T04:57:17.520Z	38.042	-121.8766667	20.006	2.17	0.43	0.29	0.18
1989-06-22T04:37:12.770Z	38.0425	-121.8893333	20.265	1.98	0.39	0.32	0.06
1989-06-22T01:13:24.190Z	38.05883	-121.8563333	19.845	4.3	0.23	0.21	
1989-06-22T01:12:02.090Z	38.0575	-121.8568333	19.155	2.73	0.27	0.23	0.12
1989-06-22T01:06:55.560Z	38.04067	-121.8921667	19.595	1.98	0.53	0.4	0.11
1989-05-28T02:52:32.770Z	38.0225	-121.8865	15.291	2.32	0.32	0.3	0.18
1989-03-30T22:33:23.490Z	37.9945	-122.0366667	16.791	2.62	0.21	0.3	0.14
1989-03-13T04:58:00.440Z	38.06617	-121.8721667	15.182	1.7	0.5	0.99	0.1
1989-02-28T06:42:48.720Z	38.20383	-121.899	4.595	2.04	2	19.25	0.17
1989-02-18T12:52:24.800Z	38.00317	-122.041	5.735	1.48	0.41	0.75	0.09
1988-11-19T21:05:05.530Z	38.22733	-121.8148333	20.679	2.16	0.54	0.55	0.16
1988-11-02T15:42:54.740Z	38.0075	-121.8708333	15.222	2	0.59	1.18	0.17
1988-06-28T02:49:14.390Z	38.2295	-121.823	17.472	2.2	0.56	0.83	0.09
1988-06-20T20:06:00.510Z	38.1235	-121.8786667	20.835	2.94	0.38	0.23	0.12
1988-06-20T05:29:19.490Z	38.1185	-121.8731667	20.726	2.06	0.63	0.38	0.07
1988-06-20T01:20:35.710Z	38.12067	-121.8618333	21.345	2.01	0.95	0.44	0.01
1988-06-20T01:15:58.300Z	38.1235	-121.8776667	20.885	3.2	0.29	0.24	0.15
1988-02-19T13:14:22.580Z	38.13767	-121.8921667	4.879	1.67	2.79	9.57	0.13
1988-01-14T09:44:00.300Z	37.99767	-121.8501667	0.522	2.14	0.44	1.2	0.27
1987-11-17T14:52:18.250Z	38.15617	-121.8625	16.975	2.86	0.33	0.38	0.21
1987-08-28T17:26:51.180Z	38.13033	-121.8838333	11.791	2.46	0.23	0.53	0.22
1987-08-10T07:49:31.350Z	38.04283	-121.885	19.699	2.02	0.35	0.47	0.14
1987-07-20T06:02:37.410Z	38.00117	-121.8518333	17.889	2.84	0.14	0.3	0.14
1987-07-16T07:54:41.080Z	38.05167	-121.8763333	16.806	2.16	0.23	0.4	0.17
1987-07-03T00:37:38.020Z	38.056	-121.8666667	18.84	2.28	0.25	0.32	0.12
1987-04-11T20:47:22.340Z	38.05917	-121.8613333	4.207	1.49	1.23	5.56	0.31
1987-02-27T07:46:45.380Z	38.13133	-122.0203333	0.045	2.14	0.83	10.96	0.41
1987-01-11T03:38:59.720Z	38.06217	-121.8635	16.05	2.88	0.22	0.45	0.15
1986-10-02T09:31:14.880Z	38.05083	-122.0025	2.303	2.11	2.05	1.24	0.47
1986-05-13T12:14:07.170Z	38.003	-121.8575	16.304	2.02	0.23	0.35	0.11
1986-04-05T17:32:42.900Z	38.17167	-121.9141667	17.4	2.52	0.4	0.35	0.25
1986-03-23T01:22:40.140Z	37.99317	-121.8576667	8.237	1.45	0.46	1.96	0.2
1986-02-24T20:33:02.950Z	38.0955	-121.9261667	5.088	1.74	1.09	30.95	0.13
1986-01-28T21:21:15.170Z	38.1385	-121.8636667	16.08	2	0.6	0.83	0.11
1985-12-20T21:30:06.490Z	38.057	-121.8846667	17.656	2	0.56	0.89	0.24
1985-11-29T01:32:25.380Z	38.25683	-121.8556667	12.527	2.12	0.75	2.03	0.1
1985-11-10T19:00:41.140Z	38.1875	-121.8735	10.817	2.15	1.71	1.98	0.1
1985-07-22T11:47:00.010Z	38.02967	-121.8775	17.536	1.94	0.47	0.3	0.2
1985-07-13T06:44:58.060Z	38.2085	-121.9781667	4.825	2.34	0.69	9.63	0.14
1985-07-12T12:37:01.560Z	38.17767	-121.9973333	0.347	2.45	0.54	4.26	0.22
1985-07-11T08:49:34.420Z	38.179	-121.9646667	2.127	2.41	0.87	7.58	0.17
1985-04-27T23:51:26.850Z	38.0145	-121.8658333	16.137	1.7	0.35	0.63	0.22
1985-03-24T01:51:52.390Z	38.0595	-121.9941667	-0.145	2.39	0.71	1.36	0.14
1985-02-05T10:21:13.930Z	38.13217	-121.9123333	16.951	2.04	0.74	0.47	0.21
1985-02-05T07:46:19.360Z	38.12233	-121.9061667	19.965	2.11	0.24	0.41	0.17

APPENDIX A.I-A. TABULATED SEISMISCITY HISTORY FOR STUDY AREA FROM 1969 TO END OF 2022

Date/time	Latitude	Longitude	Depth (km)	Magnitude	Horizontal Error (km)	Depth Error (km)	Magnitude Error
1985-02-05T04:59:30.690Z	38.12283	-121.8938333	21.645	2.14	0.43	0.37	0.18
1984-12-07T08:39:36.940Z	37.997	-121.8853333	17.188	1.89	1.22	0.62	0.26
1984-12-02T19:39:36.000Z	37.99767	-121.8313333	5.622	2.32	0.27	2.29	0.18
1984-10-28T12:13:43.940Z	38.0245	-121.8891667	15.266	1.79	0.45	0.39	0.12
1984-10-28T11:39:18.960Z	38.05583	-121.8413333	15.557	1.75	0.65	0.5	0.08
1984-10-28T11:35:46.610Z	38.06983	-121.8726667	18.12	2.84	0.29	0.25	0.13
1984-09-23T10:26:39.890Z	38.12033	-121.8771667	20.21	2.13	0.39	0.45	0.17
1984-09-21T13:47:56.400Z	38.14117	-121.8298333	4.782	1.07	58.79	59.56	0.04
1984-08-27T13:55:42.580Z	38.1265	-121.8643333	20.52	1.86	0.47	0.21	0.22
1984-08-27T06:59:18.950Z	38.14917	-121.8748333	18.68	1.52	0.64	0.76	0.29
1984-05-24T00:15:00.450Z	38.1545	-121.8781667	20.665	2.03	0.49	0.65	0.24
1984-05-05T12:43:19.170Z	38.03533	-121.8725	18.386	1.97	0.48	0.53	0.16
1984-03-20T15:57:05.640Z	38.0495	-122.0355	4.999	1.88	5.56	0.98	0.31
1984-01-28T16:02:46.220Z	38.0665	-122.0106667	-0.095	2.4	0.54	1.18	0.12
1984-01-19T23:50:43.630Z	38.20233	-121.869	9.628	2.02	0.64	1.06	0.06
1984-01-19T15:36:19.170Z	38.212	-121.885	3.648	1.9	4.5	16.68	0.14
1984-01-19T11:25:34.490Z	38.20483	-121.8556667	11.781	1.93	0.62	1.26	0.17
1984-01-18T08:11:09.600Z	38.196	-121.9021667	2.244	1.77	1.5	6.01	0.12
1984-01-18T08:10:46.200Z	38.20033	-121.8061667	15.65	2.02	0.56	0.57	0.13
1984-01-16T11:30:32.320Z	38.19867	-121.8463333	14.233	2.19	0.46	0.22	0.16
1984-01-16T11:25:39.730Z	38.212	-121.8471667	15.892	2.6	0.37	0.48	0.12
1984-01-14T16:56:09.760Z	38.05567	-121.8486667	18.01	1.7	0.47	0.34	0.17
1984-01-14T07:31:47.920Z	38.03867	-121.7756667	23.708	1.78	1.92	0.98	0.18
1983-12-18T08:14:20.810Z	38.0005	-121.8598333	3.536	1.58	0.45	1.83	0.03
1983-12-16T15:36:28.830Z	38.0615	-121.8973333	17.77	1.99	1.24	0.88	0.13
1983-11-27T09:11:28.800Z	38.1205	-121.8878333	16.762	1.97	0.55	0.42	0.22
1983-09-24T20:26:02.990Z	38.03583	-121.8765	17.11	1.92	0.71	0.84	0.03
1983-09-20T00:35:11.240Z	38.1585	-121.936	19.207	2.59	0.74	0.44	0.17
1983-09-20T00:17:28.250Z	38.18083	-121.9538333	4.717	2.05	0.56	6.26	0.17
1983-09-14T08:31:17.900Z	38.16733	-121.8646667	15.36	2.32	0.52	0.65	0.13
1983-09-14T08:09:41.430Z	38.14083	-121.89	4.78	1.25	0.81	1.35	0.27
1983-09-09T18:30:17.960Z	38.05133	-122.0406667	1.618	1.65	1.75	4.44	0.33
1983-08-30T12:33:17.500Z	38.0095	-121.895	16.186	2.15	0.25	0.32	0.16
1983-08-09T00:09:19.380Z	38.02483	-121.8935	16.89	1.53	0.64	1.3	0.07
1983-08-08T22:12:43.070Z	38.0105	-121.9023333	15.206	2.22	0.35	0.52	0.15
1983-06-29T22:46:07.770Z	38.06567	-121.8541667	14.77	1.92	0.53	1.31	0.18
1983-06-09T04:05:51.240Z	38.1365	-121.8646667	17.497	3.1	0.25	0.33	0.11
1983-06-09T03:55:48.090Z	38.11533	-121.8665	20.235	2.29	0.48	0.33	0.15
1983-06-05T11:22:43.290Z	38.03583	-121.8693333	16.917	3.5	0.21	0.33	
1983-05-06T23:14:54.830Z	38.00017	-121.9311667	15.606	2.07	0.21	0.29	0.19
1983-04-25T15:58:58.250Z	38.12883	-121.9155	4.436	0.99	3.89	7.41	
1983-03-24T15:40:00.880Z	38.041	-121.9511667	4.77	0.81	0.88	7.12	
1983-01-16T00:55:01.180Z	38.00067	-121.8576667	10.067	1.13	0.35	1.43	0.12
1983-01-10T21:37:52.370Z	38.01817	-121.9106667	4.925	1.01	23.48	36.56	0.24
1983-01-08T12:36:37.550Z	38.05467	-121.9463333	18.546	1.54	5.04	3.62	0.2
1982-12-11T21:29:32.240Z	38.07217	-121.9015	17.27	2.21	0.67	0.36	0.16
1982-12-05T20:51:48.300Z	38.0785	-121.8728333	18.65	1.65	0.94	0.92	0.16
1982-11-21T11:53:59.050Z	38.0225	-121.8626667	15.937	1.67	0.36	0.55	0.31
1982-10-20T11:47:03.260Z	38.01067	-121.855	17.157	1.47	0.52	0.65	0.19
1982-09-29T08:41:02.400Z	38.01367	-121.84	-0.21	1.33	1.42	1.71	0.29
1982-09-01T09:04:18.080Z	38.03117	-121.8853333	15.636	1.73	0.36	0.4	0.08
1982-07-25T22:45:56.800Z	38.24567	-121.6958333	14.972	1.75	0.91	1.61	0.1
1982-03-21T14:12:12.630Z	38.25283	-121.8585	15.69	1.88	0.76	1.68	0.29
1982-02-17T11:27:06.360Z	37.99933	-121.8533333	17.637	2.15	0.25	0.36	0.16
1982-02-13T03:53:06.080Z	38.1	-121.8778333	19.275	1.59	0.76	0.96	0.14

APPENDIX A.I-A. TABULATED SEISMISCITY HISTORY FOR STUDY AREA FROM 1969 TO END OF 2022

Date/time	Latitude	Longitude	Depth (km)	Magnitude	Horizontal Error (km)	Depth Error (km)	Magnitude Error
1982-02-02T02:11:43.740Z	38.01767	-121.885	16.956	2.38	0.27	0.46	0.19
1982-01-31T15:15:40.250Z	38.02817	-121.883	16.49	1.85	0.29	0.45	0.2
1982-01-31T02:58:36.880Z	38.019	-121.8811667	16.99	2.59	0.25	0.34	0.13
1982-01-25T13:31:09.360Z	37.99617	-121.8721667	5.585	2.13	0.44	9.72	0.06
1982-01-17T12:43:47.850Z	38.02583	-121.8725	17.306	2.18	0.23	0.31	0.13
1982-01-15T00:41:00.090Z	38.0105	-121.8933333	16.446	2.14	0.28	0.33	0.11
1982-01-01T14:29:01.550Z	38.094	-121.907	19.123	2.12	0.47	0.32	0.14
1981-11-18T15:32:32.170Z	38.09167	-121.873	18.346	1.99	0.36	0.44	0.18
1981-11-02T15:03:04.070Z	38.0305	-121.8731667	15.266	3.1	0.31	0.45	0.2
1981-10-18T07:24:42.630Z	38.17867	-121.9841667	6.26	1.48	0.8	20.09	0.13
1981-10-15T08:05:24.930Z	38.1195	-121.8713333	21.21	2	0.48	0.33	0.13
1981-08-12T04:17:40.490Z	38.2425	-121.9556667	4.826	1.7	0.88	15.91	0.29
1981-08-12T03:28:35.290Z	38.23433	-121.969	4.816	1.7	1.06	17.98	0.1
1981-07-26T23:46:28.570Z	38.15383	-121.862	14.88	2.27	0.41	0.7	0.14
1981-03-10T07:46:30.100Z	38.004	-121.8976667	17.946	1.76	0.39	0.71	0.18
1981-03-04T06:40:06.470Z	38.00583	-121.8995	6.226	1.46	0.43	8	0.23
1981-02-08T22:12:52.280Z	38.08817	-121.8545	16.826	1.98	0.49	0.73	0.29
1981-01-18T08:44:09.300Z	38.07483	-121.8558333	11.965	1.67	0.95	2.02	0.31
1981-01-14T13:05:00.630Z	38.02533	-121.8728333	17.237	1.75	0.61	1.33	0.17
1980-11-14T15:03:04.930Z	38.035	-121.9323333	16.686	1.51	0.41	0.38	0.05
1980-11-14T12:45:06.340Z	38.03483	-121.9355	15.816	1.71	0.26	0.46	0.19
1980-10-20T10:53:05.510Z	38.08167	-121.8728333	13.14	1.33	0.52	1.07	0.08
1980-07-20T10:31:55.870Z	38.05217	-121.871	18.246	2.24	0.32	0.45	0.09
1980-07-20T10:28:46.670Z	38.0575	-121.8591667	18.44	1.53	0.36	0.3	0.49
1980-06-28T21:26:14.210Z	38.0705	-121.8581667	18.783	1.8	0.53	0.55	0.18
1980-06-28T17:23:37.420Z	38.073	-121.8581667	21	1.58	1.01	0.81	0.05
1980-06-12T17:36:34.290Z	38.25117	-121.9563333	12.146	3.01	0.77	0.74	0.09
1980-06-09T23:40:33.620Z	38.205	-121.9625	3.439	2.43	4.67	12.67	0.07
1980-04-22T15:50:07.030Z	38.123	-121.8951667	22.742	1.72	1.77	1.64	
1980-04-15T23:49:25.340Z	38.1875	-121.9151667	10.306	1.41	3.89	3.99	0.43
1980-02-29T23:11:09.190Z	38.06833	-121.8811667	4.395	1.98	5.39	10.05	0.16
1980-02-29T23:10:08.350Z	38.09467	-121.8773333	13.376	1.94	0.66	1.14	0.09
1980-01-24T09:16:52.510Z	38.063	-121.881	18.53	2.52	0.4	0.35	0.11
1980-01-24T05:18:47.490Z	38.07083	-121.8656667	17.97	2.63	0.34	0.28	0.12
1979-12-01T02:31:07.300Z	38.00417	-121.8581667	17.257	2.35	0.22	0.25	0.08
1979-10-12T22:16:08.810Z	38.03783	-121.8735	16.326	1.94	0.38	0.57	0.14
1979-07-27T15:22:24.140Z	38.02883	-121.8628333	16.749	2.28	0.29	0.56	0.1
1979-06-25T08:10:47.940Z	38.0145	-121.863	15.076	2.02	1.25	1.12	0.12
1979-06-14T23:55:01.150Z	38.19533	-122.0338333	36.599	2.66	4.18	7.46	0.23
1979-06-04T03:15:25.150Z	37.99417	-121.867	17.482	2.24	0.78	0.57	0.21
1979-05-30T00:06:48.820Z	38.08383	-121.9551667	4.804	2.42	2.47	35.05	0.23
1979-04-25T21:19:30.710Z	38.00383	-121.8461667	16.782	2.03	0.49	0.72	0.13
1978-04-24T06:34:19.640Z	38.09217	-121.8716667	14.16	2.07	0.41	0.97	0.17
1978-03-19T16:22:09.570Z	38.04517	-121.8811667	17.466	1.83	0.37	0.43	0.2
1977-11-30T19:50:59.380Z	38.19267	-121.9193333	6.867	1.92	0.69	8.71	0.08
1977-10-06T08:39:02.600Z	38.16933	-121.9021667	19.106	2.54	0.4	0.5	0.16
1977-09-28T08:44:03.870Z	38.04767	-121.8968333	18.106	2.05	0.77	0.63	0.17
1977-09-02T14:04:13.150Z	38.11983	-121.9003333	19.067	2.23	0.52	0.92	0.18
1977-08-30T21:58:17.660Z	38.08783	-121.8688333	6.067	1.68	1.26	8.64	
1977-07-02T19:19:53.510Z	38.16967	-121.897	17.966	2.14	0.47	0.92	0.35
1977-06-17T19:59:07.630Z	38.14883	-121.8831667	20.506	1.8	0.59	0.39	0.23
1977-06-17T19:38:48.100Z	38.14633	-121.8956667	19.696	3.6	0.19	0.17	
1977-06-06T16:38:51.380Z	38.1545	-121.8951667	18.039	2.97	0.23	0.28	0.02
1977-06-06T16:17:06.790Z	38.16567	-121.883	19.906	1.88	0.62	1.06	0.01
1977-06-06T13:16:52.740Z	38.15367	-121.896	19.246	2.03	0.46	0.71	0.03

APPENDIX A.I-A. TABULATED SEISMISCITY HISTORY FOR STUDY AREA FROM 1969 TO END OF 2022

Date/time	Latitude	Longitude	Depth (km)	Magnitude	Horizontal Error (km)	Depth Error (km)	Magnitude Error
1977-06-06T12:17:39.920Z	38.15183	-121.8803333	20.827	2.11	0.91	0.56	0.23
1977-06-06T05:50:59.140Z	38.1695	-121.8916667	17.876	2.14	0.6	0.57	0.02
1977-06-06T03:41:13.740Z	38.1565	-121.8986667	17.006	1.77	0.65	1.64	0.09
1977-06-05T21:38:46.110Z	38.1485	-121.8898333	21.146	2.63	0.73	0.64	0.28
1977-06-05T16:50:57.500Z	38.16533	-121.9303333	6.376	1.73	0.94	13.79	0.04
1977-06-05T04:18:35.390Z	38.146	-121.8796667	20.446	1.81	0.48	0.36	0.16
1977-06-05T03:32:08.340Z	38.16	-121.8805	20.506	1.88	0.49	0.48	0.01
1977-06-05T01:02:47.830Z	38.14667	-121.8835	19.926	2.4	0.33	0.26	0.12
1977-06-04T22:30:29.840Z	38.17183	-121.8881667	18.956	2.04	1.15	2.23	0.18
1977-06-04T21:06:54.380Z	38.14883	-121.8973333	20.376	3.05	0.26	0.21	0.05
1977-06-04T21:00:17.590Z	38.1595	-121.8885	16.296	1.89	0.51	1.17	0.14
1977-06-04T20:57:07.230Z	38.14717	-121.8971667	20.206	3.8	0.22	0.18	
1977-06-01T13:31:32.150Z	38.1485	-121.9051667	18.636	2.13	0.33	0.48	0.12
1977-06-01T09:43:36.480Z	38.15933	-121.9023333	18.596	1.97	0.36	0.5	0.24
1977-06-01T09:38:51.440Z	38.1425	-121.9141667	21.686	2.28	0.38	0.26	0.05
1977-05-31T22:56:49.200Z	38.14667	-121.888	19.846	3.09	0.35	0.25	0.07
1977-05-16T00:12:28.720Z	38.1515	-121.9406667	6.441	1.65	0.51	9.71	0.09
1977-05-15T19:28:19.140Z	38.14783	-121.9108333	20.667	2.7	0.49	0.41	0.07
1977-05-11T17:17:36.960Z	38.153	-121.8968333	17.686	1.74	0.51	0.62	0.2
1977-05-08T06:29:09.290Z	38.14833	-121.8938333	20.206	2.76	0.27	0.21	0.04
1977-05-06T16:58:32.130Z	38.14767	-121.8785	20.056	1.99	0.52	0.48	0.1
1977-05-06T15:54:13.780Z	38.15233	-121.8793333	20.396	2.25	0.63	1.05	0.19
1977-05-06T09:27:31.290Z	38.16317	-121.8978333	18.246	2.15	0.32	0.56	0.08
1977-05-06T04:41:00.200Z	38.15167	-121.9505	-0.049	1.79	0.97	7.16	0.14
1977-05-05T22:43:23.660Z	38.15833	-121.9255	18.506	2.19	0.57	0.33	0.08
1977-05-05T22:40:31.170Z	38.14717	-121.8926667	20.166	3.3	0.2	0.17	
1977-05-05T06:37:33.150Z	38.1535	-121.8831667	20.3	2.62	0.43	0.28	0.12
1977-05-05T04:31:04.340Z	38.14517	-121.9081667	20.886	2.38	0.44	0.34	0.12
1977-05-04T19:43:33.140Z	38.14867	-121.892	20.336	3.2	0.32	0.23	
1977-04-13T00:12:13.900Z	38.126	-121.8763333	20.846	2.33	0.9	0.48	0.09
1977-04-13T00:00:11.730Z	38.12883	-121.8818333	22.726	2.36	0.94	0.39	0.1
1977-04-06T04:49:17.030Z	38.095	-121.8396667	19.556	2.3	0.56	0.5	0.09
1977-03-15T21:24:00.310Z	38.128	-121.9028333	19.491	2.86	0.27	0.46	0.07
1976-11-17T05:34:09.810Z	38.2145	-121.865	19.692	2.53	0.48	0.17	0.02
1976-11-15T09:27:28.480Z	38.20533	-121.8438333	19.397	2.79	0.77	0.53	0.15
1976-11-15T08:33:59.530Z	38.2085	-121.8701667	20.106	2.54	0.37	0.45	0.22
1976-11-15T05:58:53.510Z	38.20183	-121.8445	19.421	3.24	0.35	0.4	0.05
1976-11-12T13:32:00.550Z	38.202	-121.8586667	25.276	2.2	1.41	1.01	0.35
1976-11-07T00:38:03.820Z	38.20683	-121.8873333	21.777	2.15	0.43	0.62	0.16
1976-08-23T20:51:20.770Z	38.08667	-121.8551667	19.196	3.15	0.71	0.47	0.06
1976-07-28T12:11:02.310Z	38.04117	-121.8471667	5.037	2.91	4.4	16.27	0.03
1976-07-20T13:13:10.810Z	38.04033	-121.884	15.877	2.31	0.46	0.39	0.09
1976-07-13T13:34:52.990Z	38.07	-121.87	4.796	3.4	0.67	4.02	
1976-05-03T05:42:38.470Z	38.10717	-121.8736667	20.277	3.4	0.4	0.29	
1976-03-21T14:49:13.320Z	38.07583	-121.8988333	18.316	2.27	0.37	0.5	0.23
1976-02-23T20:03:29.880Z	38.108	-121.8653333	4.621	1.74	1.59	9.52	
1975-11-30T02:12:26.570Z	38.06117	-121.8903333	17.826	2.22	0.53	0.47	0.37
1975-11-26T13:03:06.470Z	38.09117	-121.853	14.096	1.96	0.82	1.09	0.14
1975-10-27T23:43:28.880Z	38.09117	-121.8966667	14.949	2.32	0.33	0.63	0.3
1975-07-24T23:00:46.100Z	38.01433	-121.8551667	16.497	2.26	0.36	0.56	0.12
1975-07-13T13:22:43.180Z	38.06567	-121.8711667	9.109	1.9	0.31	1.15	0.17
1975-06-17T05:27:07.630Z	38.043	-121.8621667	17.857	3.5	0.32	0.32	
1975-06-12T09:39:09.500Z	38.00867	-122.0105	20.043	1.59	1.41	0.85	0.13
1975-06-07T06:38:47.180Z	38.1125	-121.8983333	19.952	2.47	0.37	0.3	0.1
1975-05-26T19:50:50.410Z	38.003	-121.8543333	17.082	2.61	0.39	0.26	0.15

APPENDIX A.I-A. TABULATED SEISMISCITY HISTORY FOR STUDY AREA FROM 1969 TO END OF 2022

Date/time	Latitude	Longitude	Depth (km)	Magnitude	Horizontal Error (km)	Depth Error (km)	Magnitude Error
1974-08-04T03:43:53.450Z	37.99933	-121.8451667	18.237	3	0.3	0.24	
1974-04-22T14:26:18.530Z	38.03	-121.9823333	15.402	2.49	0.6	0.79	0.2
1974-04-21T05:49:45.020Z	38.119	-121.8951667	21.276	2.28	0.43	0.51	0.06
1974-04-21T01:28:41.960Z	38.12567	-121.8906667	21.096	1.98	0.52	0.59	0.26
1974-03-21T06:47:33.010Z	38.10633	-121.9841667	20.63	1.73	0.84	1.64	0.25
1974-03-16T06:39:13.720Z	38.06567	-121.8885	16.671	1.81	0.4	0.64	0.3
1974-02-15T18:57:04.710Z	38.04617	-121.8496667	11.653	2.36	0.54	1.46	0.7
1974-02-11T07:14:25.480Z	38.06267	-121.9005	5.915	1.82	0.73	9.68	0.08
1974-01-28T06:15:20.820Z	38.10767	-121.8975	16.232	1.93	0.67	1.64	0.25

Note:
Source is April 24, 2024 download from the USGS Advanced National Seismic System (ANSS) Comprehensive Earthquake Catalog (ComCat).